

2

AD-A247 016



Report No. NADC-91113-50



FUNDAMENTAL NOISE LIMITS IN MINIATURE ACOUSTIC AND VIBRATION SENSORS

Thomas B. Gabrielson
Mission Avionics Technology Department (Code 5044)
NAVAL AIR DEVELOPMENT CENTER
Warminster, PA 18974-5000

31 DECEMBER 1991

PHASE REPORT
Program Element No. 0602314N
Project No. NA3A
Task No. RJ14K14.1
Work Unit No. 100083

DTIC
ELECTE
MAR 05 1992
S D D

Approved for Public Release; Distribution is Unlimited

Prepared for
OFFICE OF NAVAL TECHNOLOGY
Chief of Naval Research
800 N. Quincy Street
Arlington, VA 22217-5000

92 3 03 144

92-05697

NOTICES

REPORT NUMBERING SYSTEM -- The numbering of technical project reports issued by the Naval Air Development Center is arranged for specific identification purposes. Each number consists of the Center acronym, the calendar year in which the number was assigned, the sequence number of the report within the specific calendar year, and the official 2-digit correspondence code of the Command Officer or the Functional Department responsible for the report. For example: Report No. NADC-88020-60 indicates the twentieth Center report for the year 1988 and prepared by the Air Vehicle and Crew Systems Technology Department. The numerical codes are as follows:

CODE	OFFICE OR DEPARTMENT
00	Commander, Naval Air Development Center
01	Technical Director, Naval Air Development Center
05	Computer Department
10	AntiSubmarine Warfare Systems Department
20	Tactical Air Systems Department
30	Warfare Systems Analysis Department
40	Communication Navigation Technology Department
50	Mission Avionics Technology Department
60	Air Vehicle & Crew Systems Technology Department
70	Systems & Software Technology Department
80	Engineering Support Group
90	Test & Evaluation Group

PRODUCT ENDORSEMENT — The discussion or instructions concerning commercial products herein do not constitute an endorsement by the Government nor do they convey or imply the license or right to use such products.

Reviewed By: *London Marshall* Date: 27 Jan 92
Branch Head

Reviewed By: *Jim M. Ambrose* Date: 1/28/92
Division Head

Reviewed By: *W. C. Stoddard* Date: 1/31/92
Director/Deputy Director

REPORT DOCUMENTATION PAGE

Form Approved
OMB No. 0704-0188

Public reporting burden for this collection of information is estimated to average 1 hour per response, including the time for reviewing instructions, searching existing data sources, gathering and maintaining the data needed, and completing and reviewing the collection of information. Send comments regarding this burden estimate or any other aspect of this collection of information, including suggestions for reducing this burden, to Washington Headquarters Services, Directorate for Information Operations and Reports, 1215 Jefferson Davis Highway, Suite 1204, Arlington, VA 22202-4302, and to the Office of Management and Budget, Paperwork Reduction Project (0704-0188), Washington, DC 20503.

1. AGENCY USE ONLY (Leave blank)		2. REPORT DATE 31 December 1991	3. REPORT TYPE AND DATES COVERED Phase	
4. TITLE AND SUBTITLE Fundamental Noise Limits in Miniature Acoustic and Vibration Sensors			5. FUNDING NUMBERS Program Element 0602314N Project No. NA3A Task No. RJ14K14.1 Work Unit No. 100083	
6. AUTHOR(S) Thomas B. Gabrielson				
7. PERFORMING ORGANIZATION NAME(S) AND ADDRESS(ES) Mission Avionics Technology Department (Code 5044) NAVAL AIR DEVELOPMENT CENTER Warminster, PA 18974-5000			8. PERFORMING ORGANIZATION REPORT NUMBER NADC-91113-50	
9. SPONSORING/MONITORING AGENCY NAME(S) AND ADDRESS(ES) OFFICE OF NAVAL TECHNOLOGY Chief of Naval Research 800 Quincy Street Arlington, VA 22217-5000			10. SPONSORING/MONITORING AGENCY REPORT NUMBER	
11. SUPPLEMENTARY NOTES				
12a. DISTRIBUTION/AVAILABILITY STATEMENT Approved for Public Release; Distribution is Unlimited			12b. DISTRIBUTION CODE	
13. ABSTRACT (Maximum 200 words) Conventional noise analysis for acoustic and vibration sensors has focused either on the ambient noise floor imposed by the environment or the electrical noise floor imposed by the preamplifier. Microminiature sensors are, however, particularly sensitive to thermal (molecular) agitation because of their small moving parts. This mechanical-thermal noise can easily dominate the noise performance of these sensors. The purposes of this report are to review the fundamental noise sources in a sensor system and to illustrate the importance of noise sources intrinsic to the sensor's design. In particular, thermal noise, shot noise, 1/f noise, and amplifier noise components are discussed as they relate to the sensor system.				
14. SUBJECT TERMS Thermal noise, shot noise, 1/f noise, micromachined sensors, miniature sensors, sensor preamplifiers			15. NUMBER OF PAGES	
			16. PRICE CODE	
17. SECURITY CLASSIFICATION OF REPORT Unclassified	18. SECURITY CLASSIFICATION OF THIS PAGE Unclassified	19. SECURITY CLASSIFICATION OF ABSTRACT Unclassified	20. LIMITATION OF ABSTRACT UL	

**Fundamental Noise Limits
in Miniature Acoustic and Vibration Sensors**

Thomas B. Gabrielson

Introduction.....1
 Thermal Noise.....4
 Quality factor.....9
 The simple accelerometer.....11
 The simple pressure sensor.....15
 Dissipation mechanisms.....16
 Noise estimation from sensor response.....21
 Sensors with feedback.....23
 Compound sensors.....26
 Limits of applicability.....28
 Shot Noise.....29
 1/f Noise.....33
 Amplifier Noise.....36
 Equivalent input noise sources.....37
 Operational amplifiers with feedback.....41
 General considerations for preamplifiers.....46
 Summary.....47
 Appendix A. Derivation of Nyquist's Relation.....48
 Appendix B. Equivalent-Circuit Modeling with SPICE.....51
 Appendix C. Noise analysis of Op Amps and JFETs.....62
 Appendix D. Electromechanical Transducer Equivalents.....73
 Appendix E. Radiation Loading of Transducers.....84
 References.....86



Accession For	
NTIS CRA&I	<input checked="" type="checkbox"/>
DTIC TAB	<input type="checkbox"/>
Unannounced	<input type="checkbox"/>
Justification	
By	
Distribution /	
Availability Codes	
Dist	Avail and/or Special
A-1	

Introduction

Since the introduction of the micromachining process, wherein mechanical structures are etched from blocks of silicon, a number of very small acoustic and vibration sensors have been built (for example, [1-7]). Ranging from simple capacitive pressure sensors [8] to accelerometers that measure the proof-mass displacement by electron tunneling with active mechanical feedback [9], these sensors are attractive for many space-limited applications. However, the small moving parts are especially susceptible to mechanical noise resulting from molecular agitation. If the sensor is intended for low-level signals, this mechanical-thermal noise can be the limiting noise component.

Because mechanical-thermal noise has not been important for conventionally sized sensors, the analysis procedures are often unfamiliar and the mechanism is often neglected. Many designers fall into the trap of making elaborate analyses of more common but less important sources of noise. The purpose of this paper is to present some simple techniques for evaluating mechanical-thermal noise limits and to review shot, $1/f$, and amplifier noise. While these techniques are especially useful for designing microminiature sensors, the principles are generally applicable for any sensor intended for extreme sensitivity.

The basic types of noise considered are:

Thermal Noise: The random fluctuations result from molecular vibration.

This component is called Johnson Noise in electrical systems and Brownian Motion in mechanical systems.

Shot Noise: The noise associated with random emission of particles (or photons) that have not yet reached thermal equilibrium with their surroundings. Examples are emission of photons from a laser and transit of charge carriers across a semiconductor junction.

1/f Noise: A frequently observed noise component with power that decreases roughly linearly with increasing frequency (roughly equal power per octave). As yet, there is no satisfactory physical model for 1/f noise. This type of noise makes DC and very low frequency measurements difficult. It is also called flicker noise or excess noise.

Since both mechanical, electrical, and thermodynamic quantities will be used in these notes, any system of units other than SI would make calculations awkward and prone to error. Consequently, SI units will be used throughout: temperature in kelvin (K), mass in kilograms (kg), and length in meters (m). One point of caution: these units lead to a base unit of pascal (Pa) for pressure while the standard reference for underwater acoustics is the micropascal (μPa). Also, a common unit for acceleration is the "g" but the SI unit is m/s^2 ; one g is 9.8 m/s^2 .

All of these noise quantities are distributed in frequency so they are usually given in terms of spectral density: some quantity (proportional to power) per hertz. Some examples of the units are: volts^2/Hz , m^2/Hz , g^2/Hz , $\mu\text{Pa}^2/\text{Hz}$. These are frequently expressed in terms of the linear quantities as follows: $\text{volts}/\sqrt{\text{Hz}}$, $\text{m}/\sqrt{\text{Hz}}$, $\text{g}/\sqrt{\text{Hz}}$, $\mu\text{Pa}/\sqrt{\text{Hz}}$. These linear units should be used with caution because, when individual noise sources are incoherent, as is most often the case, their powers add, not their voltages. To adjust for a known frequency band, multiply the power-like quantity (volts^2/Hz , for example) by the bandwidth; or, multiply the linear quantity ($\text{volts}/\sqrt{\text{Hz}}$, for example) by the square root of the bandwidth.

In order for a noise analysis to have practical value, the results need to be compared to the desired sensitivity of the sensor. In underwater acoustics, a reasonable choice for the desired minimum signal to be measured is the quietest level of ocean background noise. Table I gives an approximation to these levels from 0.1 to 1000 Hz. The values were obtained by subtracting 10 dB from an average quiet-ambient curve [10]. Notice that the acoustic displacements are very small; the displacement at 1000 Hz is about equal to the diameter of a proton! The pressure and the acceleration corres-

ponding to this SSO-10dB ("sea-state zero minus 10 dB") curve are shown in Figure 1 and tabulated in Table I. In practice, each sensor application must be examined individually to determine the minimum signal requirement; in these notes, however, the SSO-10dB curve will be used to illustrate the analysis.

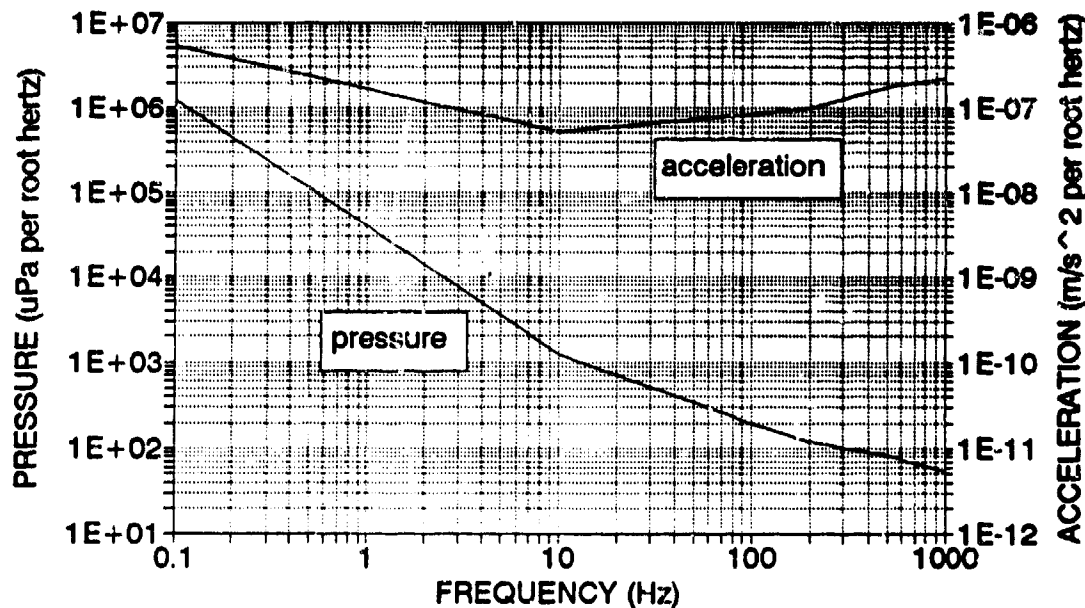


Figure 1. Acoustic pressure and particle acceleration corresponding to Sea State Zero minus 10 dB.

Table I. Sea State Zero - 10 dB

FREQUENCY	LEVEL	PRESSURE	VELOCITY	DISPLACEMENT	ACCELERATION
(f)	(NL)	(p)	(v)	(x)	(a)
Hz	dB	uPa prH	m/s prH	m prH	m/s ² prH
0.1	122	126000	8.4E-07	1.5E-06	5.3E-07
1	92	4000	2.7E-08	4.2E-09	1.7E-07
10	62	1260	8.4E-10	1.3E-11	5.3E-08
100	46	240	1.3E-10	2.1E-13	8.4E-08
1000	34.5	53	3.5E-11	5.6E-15	2.2E-07

Notes: Level (NL) is in db//uPa² per hertz
 "prH" stands for per root hertz

NADC-91113-50

(The various acoustic amplitudes are related as follows:

$$\begin{aligned} p &= 10^{NL/20} \text{ in } \mu\text{Pa}/\sqrt{\text{Hz}} \\ v &= (p/10^5)/\rho c \text{ (note conversion to Pa;} \\ &\quad \rho c = 1\,500\,000 \text{ kg/m}^2\text{s);} \\ x &= v/\omega \text{ where } \omega = 2\pi f \\ a &= v\omega \end{aligned}$$

For audio microphone design, ambient levels are often expressed as A-weighted levels [11] (where the reference level is 20 μPa not 1 μPa). The equivalent bandwidth for a source of white noise (uniformly distributed in frequency) is roughly 15 000 Hz; noise spectral density values can be converted to A-weighted levels by multiplying the per hertz value by 15 000 Hz and then dividing by 400 (20 μPa squared). If the noise spectral density is given in dB with respect to 1 μPa^2 per hertz, the value can be converted to A-weighted level by adding 16 dB. Some typical background levels [11, 12] are: 25-30 dB(A) in recording studios, 35-40 dB(A) in churches, and 30-50 dB(A) in quiet residential areas

Thermal Noise

The concept of thermal equilibrium [13] is generally taught in basic thermodynamics courses: A collection of molecules reaches equilibrium in which each molecule has, on average, the same amount of energy. If another molecule is added to the "bath," it too reaches the same average energy level after a few collisions. What is not often appreciated is that this uniform distribution of energy applies to macroscopic objects also. A golf ball placed in that molecular bath will, after many collisions, acquire an average kinetic energy equal to that of any of the molecules. The only difference is that it takes a substantially greater number of collisions to bring the golf ball into thermal equilibrium [14].

One of the more well known mechanisms for mechanical-thermal noise is Brownian Motion [15]. Here, the agitation of an observable object is caused

by molecular collisions from a surrounding gas or liquid and the agitation is directly related to the fluid's viscosity. In fact, any molecular agitation even through solid structures like springs and supports can cause movement of an object and each fluctuation component is related to a mechanical damping.

Compare the lossless harmonic oscillator with the damped harmonic oscillator in Fig. 2.

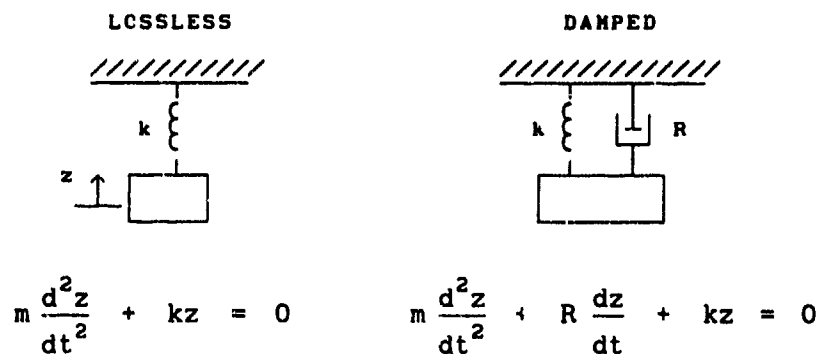


Figure 2. Lossless and damped simple harmonic oscillators.

The presence of damping in the system on the right suggests that any oscillation would continue to decrease in amplitude forever. Even the small, random jitter caused by molecular motion would decay; this, however, is the same thing as saying that the temperature (a measure of this molecular motion) would continually decrease. The temperature cannot drop below that of the surroundings so the model on the right violates the Second Law of Thermodynamics. For mechanical systems, this is not normally a problem but, if a sensor is being designed for very small signals, the excitation of the oscillator by molecular vibration can be significant.

The correct physical model for the damped simple harmonic oscillator includes a force generator of sufficient amplitude to bring the system into thermal equilibrium rather than to let it decay to the equivalent of absolute zero temperature. The proper differential equation is:

$$m \frac{d^2 z}{dt^2} + \underbrace{R \frac{dz}{dt} + k z}_{\quad} = \underbrace{f_n(t)}_{\quad} \quad (1)$$

where f_n is the fluctuating force required to maintain thermal equilibrium. The presence of the damping term in the equation requires that the fluctuating force be present as well. *This is a crucial relationship.*

Since noise sources add incoherently (power adds, not force), the forcing power should be linear with R. Also, the energy in molecular vibrations is a linear function of temperature, so the forcing power should also be linear with T. Consequently, the force should be proportional to the square root of R times T.

The association between damping and fluctuation is expressed by the *Fluctuation-Dissipation Theorem* [16]: any mechanism for dissipation causes fluctuations. If there is a path for energy to leave an object or system, then that path also allows thermally excited molecules in the environment to transfer disordered, fluctuating energy to the object. This "dissipation" can represent any mechanism that would cause the oscillation to decay: mechanical damping, acoustic or electromagnetic radiation, transfer of power to a load.

The basic relationship that governs thermal noise analysis is expressed by the *Equipartition Theorem* [13, 14, 17]: any "mode" of a system in thermal equilibrium has an average noise energy of $\frac{1}{2}k_B T$ where k_B is Boltzmann's constant (1.38×10^{-23} J/kelvin) and T is the absolute temperature (here in kelvin: $K = ^\circ C + 273$). The modes of the system can be identified by writing out all of the components of the system energy. Any component that depends on the square of a coordinate is a mode in the above sense. Common examples include kinetic energy ($\frac{1}{2}mv^2$), spring potential energy ($\frac{1}{2}kx^2$), energy stored in a capacitor ($\frac{1}{2}CV^2$), and energy stored in an inductor ($\frac{1}{2}LI^2$). Equipartition claims that the thermal energy is equally distributed among all the energy storage modes and, furthermore, is equal to $\frac{1}{2}k_B T$ for each mode.

The key to analyzing mechanical systems in equilibrium is that simple equipartition holds for every mode of energy storage (as long as $k_B T \gg hf$ where h is Plank's constant, 6.6×10^{-34} Js, and f is frequency). Each mode (kinetic or potential), whether corresponding to an observable motion of a macroscopic mass or microscopic motion of molecular motion, vibration, or rotation, has the same amount of thermal energy and these modes are continually exchanging energy with all of the other modes in order to maintain this equilibrium.

If an "ordered" mode such as the vibration of a macroscopic mass-spring system is in equilibrium with a large number of independent microscopic modes (say, individual molecular vibrations in the spring), then an observable "dissipation" results [18]. Energy from the orderly motion of the mass-spring system is transferred (at some measureable rate) to a very large number of molecular modes. In turn, the molecular vibrational modes transfer energy back to the mass-spring oscillator; however, since the molecular vibrations are essentially independent of each other, the return transfers are random and the probability of them being in phase enough to reinforce the mass-spring motion is effectively zero. So the whole system (mass-spring vibrator and molecules in the spring), if no longer driven externally, eventually reaches a state where the energy in the mass-spring motion equals the energy in any of the many molecular vibrations.

The principle of equipartition leads directly to the first technique for analyzing mechanical-system noise [19]. The average displacement of the mass in a mass-spring oscillator is given by

$$\boxed{\frac{1}{2} k \langle x^2 \rangle = \frac{1}{2} k_B T} \quad (2)$$

Here, $\langle \rangle$ denotes an average and it is a broadband average. Also, k is the

spring constant while k_B is Boltzmann's constant. The average velocity of the mass is

$$\frac{1}{2} m \langle v^2 \rangle = \frac{1}{2} k_B T \quad (3)$$

A free particle (an atom of Helium gas, for example) may not have a spring-like storage mode but its kinetic energy is still subject to equipartition. Since the three coordinate directions are independent, there are three kinetic modes. The x, y, and z components each have an average kinetic energy of $\frac{1}{2} m \langle v_x^2 \rangle = \frac{1}{2} k_B T$ so the total average energy of the particle is $\frac{3}{2} k_B T$.

In some analyses, these simple relations will suffice but, often, the frequency distribution of the noise is required. In this case, the noise response of a device can be calculated by inserting a force generator at the same location as each damper in the system. The spectral density of the force corresponding to each damper is (see Appendix A)

$$F_n = \sqrt{4k_B TR} \quad [N/\sqrt{Hz}] \quad (4)$$

This result is derived directly from equipartition: a system mode having $\frac{1}{2} k_B T$ broadband energy is equivalent to the damper having an associated force generator with $\sqrt{4k_B TR}$ spectral density. (The damping coefficient R is mechanical resistance — force per velocity — and can be a function of frequency. To analyze electrical systems, put a voltage generator of $\sqrt{4k_B TR}$ volts/ \sqrt{Hz} in series with each resistor in the circuit. Here, R is electrical resistance [20, 21].)

One of the consequences of the Fluctuation-Dissipation theorem is that, if the dissipation (loss, damping, resistance) of a system is measured, the individual contributors to that dissipation need not be known: it is the total dissipation acting on a mass-spring oscillator that determines the thermal fluctuations of that oscillator. This is why a measurement of the Q of an

oscillatory system is useful in noise analysis: the measured Q incorporates all of the dissipation mechanisms that are acting on the system.

Another consequence of the F-D relations is that individual dampers can be treated individually if that is more convenient. This is particularly useful in modeling devices. Construct the equivalent circuit for the entire device (include both mechanical and electrical parts) and, for each resistance, add a series force (or voltage) generator of magnitude $4k_B TR$ (newtons or volts per root hertz). Calculate the system output resulting from each of these noise generators separately and then sum the squares of these individual outputs to get the square of the total noise output.

Quality Factor

Since mechanical damping is a critical part of thermal noise analysis, it is useful to have several ways of determining it. In some cases, the mechanical resistance can be modeled fairly accurately (for example, viscous drag on simple shapes at low Reynolds numbers), but in others it must be measured. For simple harmonic oscillators the quality factor or Q is related to the damping and can often be measured easily. Several expressions of Q are useful:

- (1) Q is 2π times the number of cycles of oscillation required for the energy of the oscillator to drop by the factor e:

$$E(t) = E_0 \exp(-\omega_0 t/Q) \quad (5)$$

- (2) Q is the ratio of the resonance frequency to the full width of the resonance peak at the half-power points (3 dB down points):

$$Q = f_0 / \Delta f_{3dB} \quad (6)$$

- (3) Q is the ratio of either the mass reactance or the stiffness reactance at resonance to the resistance in a series resonant circuit:

$$Q = \omega_0 m / R = k / \omega_0 R \quad (7)$$

NADC-91113-50

(4) Q equals 2π times the energy stored in the oscillator divided by the energy dissipated per cycle. Q is also equal to ω_0 times the energy stored in the oscillator divided by the power dissipated.

(5) Q is related to the damping factor ζ or the loss tangent

$$Q = 1/(2\zeta) = 1/\tan\delta \quad (8)$$

Critical damping ($R = 2m\omega_0$) is $\zeta = 1$ or $Q = 1/2$.

(6) When the Q is small, methods (1) and (2) are not very useful. In this case, the resonance frequency can be measured by exciting the system and looking for the frequency that results in a 90 degree phase shift between the input and output. The damping can be determined from the slope of the phase change (in radians per hertz) at the resonance:

$$Q = f_0 \left(\frac{d\phi}{df} \right)_{f_0} / 2 \quad (9)$$

(7) Another approach for small Q is to drive the system with a square wave. The output waveform will show "ringing" at the level transitions. If the peak-to-trough amplitude, a, of the first half cycle of the ringing and the trough-to-peak amplitude, b, of the second half cycle are measured, then the damping factor can be computed as follows [22, 23]:

$$\zeta = \frac{\ln(a/b)}{\sqrt{\ln^2(a/b) + \pi^2}} \quad (10)$$

The Simple Accelerometer

The generic accelerometer sensor is shown schematically in Fig. 3. The case is exposed to the desired acceleration and the displacement of the mass relative to the case ($z = y - x$) is the output of the accelerometer. Also shown are the location of the noise force, and the free-body diagram.

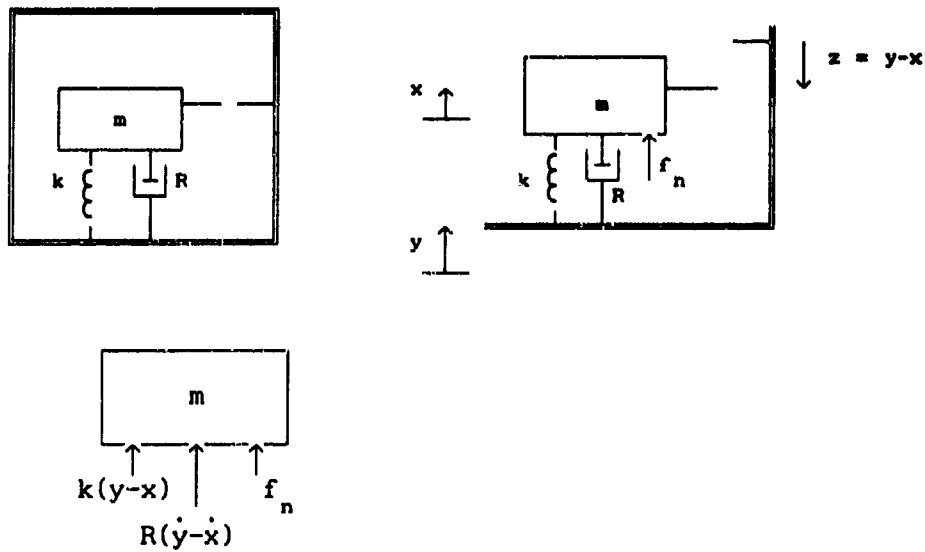


Figure 3. Configuration and free-body diagram for simple accelerometer.

Of course, the noise force also acts on the sensor case through the other end of the damper but this is not important here. The analysis is simpler in the frequency domain where the signal excitation displacement is $Y(f)$, the response is $Z(f)$, and the noise force is F_n . (As a reminder, $y \rightarrow Y$, $\dot{y} \rightarrow i\omega Y$, and $\ddot{y} \rightarrow -\omega^2 Y$ in the frequency domain.) To get the noise response, set the signal Y to zero and solve for Z_n in terms of F_n ; to get the signal response, set F_n to zero and solve for Z_s in terms of the case displacement Y .

Solving the simple accelerometer for the noise response gives

$$|Z_n(f)| = \sqrt{4k \frac{TR}{B}} G(f) / k \quad (11)$$

where

$$G(f) = 1 / \sqrt{[1 - (f/f_0)^2]^2 + (f/f_0)^2/Q^2} \quad (12)$$

and $4\pi^2 f_0^2 = \omega_0^2 = k/m$. The factor $G(f)$ is plotted in Figure 4 for Q 's of 0.5, 4, and 100.

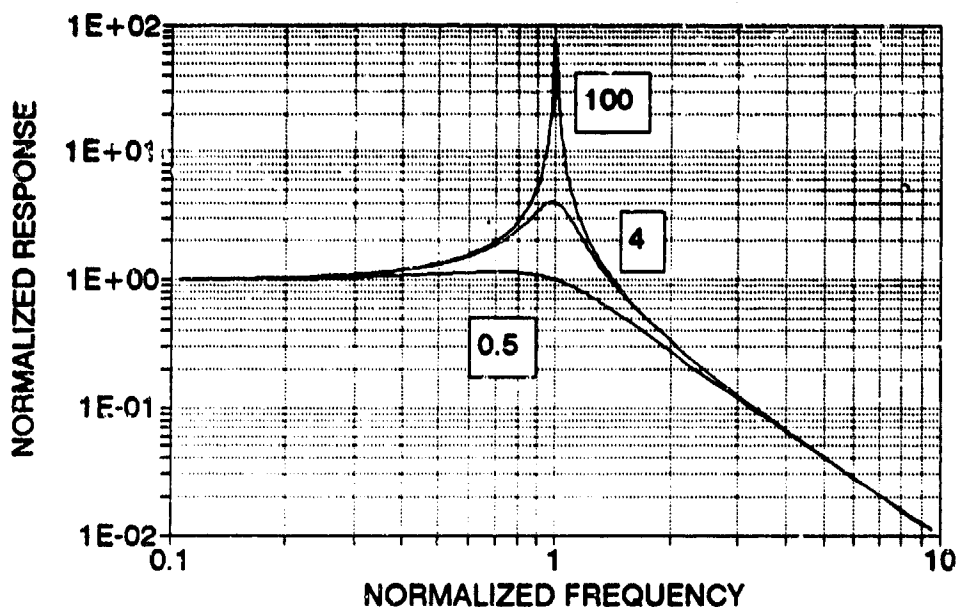


Figure 4. Normalized response, $G(f)$, of a mass-spring oscillator as a function of normalized frequency, f/f_0 , for three values of Q .

In the accelerometer limit ($f \ll f_0$), the noise displacement becomes

$$|Z_n(f)| = \sqrt{4k_B T R} / k \quad (13)$$

which can also be expressed in terms of the Q of the oscillator:

$$|Z_n(f)| = \sqrt{4k_B T / \omega_0^2 k} = \sqrt{4k_B T / \omega_0^3 m Q} \quad (14)$$

The signal response is

$$|Z_s(f)| = (f/f_0)^2 G(f) |Y_s| \quad (15)$$

but $\omega^2 |Y_s|$ is the magnitude of the input acceleration, a_s , so

$$|Z_s(f)| = a_s G(f) / \omega_0^2 \quad (16)$$

and $G(f)$ is one in the accelerometer limit.

The signal-to-noise ratio at any frequency is then

$$\boxed{|Z_s / Z_n|^2 = a_s^2 m Q / 4k_B T \omega_0} \quad (17)$$

(Note: a moving-coil accelerometer has its electrical output proportional to dz/dt or ωZ ; this is true for both signal and noise however, so the signal-to-noise ratio is unchanged.) Here, the "signal" is taken to be the power spectral density of the ambient noise of the environment. This is appropriate for a sensor designed for optimum reception of real signals in this ambient; if, however, the real signals are guaranteed never to approach the environmental ambient, then the minimum real signal level should be used. (That could be a single-frequency level rather than a spectral density in which case the noise power should be adjusted by the analysis bandwidth.)

From this expression for signal-to-noise ratio it is apparent that the SNR can be improved by:

- (1) increasing the Q
- (2) reducing ω_0
- (3) increasing m (which also lowers ω_0)
- (4) reducing the stiffness (which lowers ω_0)

Normally, dropping ω_0 far enough so that it is within the band of expected signals is not wise because this introduces a nonlinear phase into the system response. Increasing the Q can cause problems also: if the oscillator has a high Q , then out-of-band oscillations can be large (at the resonance frequency, Q times the motion well below the resonance for the same excitation) and the mechanical system must have enough dynamic range to handle these large movements. As will be discussed later, feedback can be applied to reduce the mechanical range required but then feedback circuit must have an

adequate dynamic range. Moreover, the feedback circuit introduces additional noise.

Example 1. Determine the thermal noise limit for a critically damped accelerometer that must be sensitive enough to detect the SS0-10dB levels from 0.1 to 1000 Hz. Assume that an SNR > 1 is adequate. (Unless otherwise stated, all accelerometer-type hydrophones will be assumed to be neutrally buoyant so that the fluid acceleration equals the sensor acceleration.)

The lowest practical resonance frequency is 1000 Hz and the Q is 1/2 for critical damping. The smallest acceleration to be measured (see Table I) is 5.3×10^{-8} m/s² per $\sqrt{\text{Hz}}$, which occurs at 10 Hz. In order to have an SNR > 1 at 10 Hz, the mass must be greater than 72 grams (from Eq. 17). Clearly, this would be a problem for a very small sensor.

Critical damping gives good response linearity at the expense of thermal noise. If the Q were raised to 100, the minimum mass drops to 0.36 gm. If the Q were kept at 1/2 but the resonance were dropped to 10 Hz, the minimum mass drops to 0.72 gm. In this latter case, however, the signal response now rolls off above 10 Hz. This is not a problem for mechanical thermal noise since the SNR is not a function of frequency, but this would be a dangerous strategy since other noise sources could eventually dominate.

Example 2. What is the minimum Q required for a simple accelerometer with $m = 40 \times 10^{-6}$ kg and $f_0 = 300$ Hz so that thermal noise is at or below SS0-10dB from 0.1 Hz to f_0 ?

Smallest SS0-10dB acceleration is at 10 Hz so SNR must be one or greater at 10 Hz. From Eq. 17, the Q must be at least 270. If the mass were reduced to 2×10^{-6} kg, then the minimum Q would be 5400! This illustrates one of the problems associated with miniature accelerometers.

The Simple Pressure Sensor

In the simple pressure sensor, the moving mass is directly exposed to the incident acoustic pressure and the displacement (or speed) of this mass is measured. Such a sensor is shown in Fig. 5.

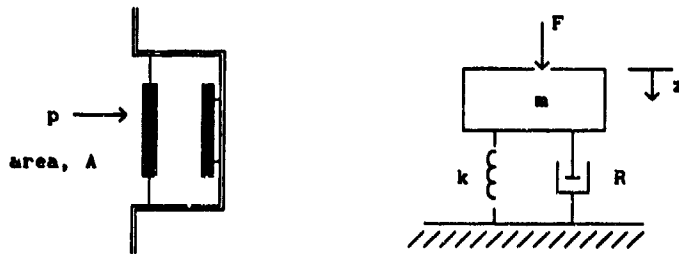


Figure 5. Schematic diagram of a simple pressure sensor.

For an arbitrary force F , the displacement response Z is

$$|Z| = F G(f) / k \tag{18}$$

For signal, the force $F = p_s S$, where S is the area of the transducer face and p_s is the spectral density of the signal pressure; for noise, the force $F = \sqrt{4k_B T R}$, so the signal-to-noise ratio is

$$\boxed{|Z_s / Z_n|^2 = (p_s S)^2 / 4k_B T R = Q(p_s S)^2 / 4k_B T \omega_0 m} \tag{19}$$

In this case, the signal-to-noise ratio can be improved by:

- (1) increasing the area, A
- (2) increasing Q
- (3) reducing the resonance frequency
- (4) reducing the mass (unless the stiffness is also reduced this increases ω_0 since $\omega_0^2 = k/m$)

Reduction of the mass would seem to favor microminiaturization but the $\omega_0 m$ product goes as \sqrt{m} , which makes this dependence weak, whereas the dependence on area is as area squared.

Example 3. Design a critically damped pressure sensor with thermal noise at or below the SS0-10dB curve from 0.1 to 1000 Hz if the sensor area is 1 cm^2 .

Here Q is $1/2$. Set f_0 to 1000 Hz (lowest value without dropping resonance into desired band). The worst case for pressure on the SS0-10dB curve is at 1000 Hz where $p_n = 53 \mu\text{Pa}/\sqrt{\text{Hz}}$. From Eq. 19, the mass must be less than 140 grams. (Be careful with units: use pressure in pascals, not micropascals, in Eq. 19.) If the sensor area were reduced to 1 mm^2 , then the mass would have to be less than 14 *micrograms*. Also, the stiffness would have to be reduced to keep the resonance at 1000 Hz.

One of the advantages of working with the Q of a sensor is that, if the Q is measured, it automatically includes all of the relevant damping terms. While this is only strictly true for single-degree-of-freedom systems with frequency-independent resistance, many sensors can be approximately modeled this way. In order for a Q measurement to be useful, though, the Q must be measured with the sensor in the environment in which it will ultimately be used. For example, the Q of a hydrophone should be measured in water, not in air. Sometimes the difference may be negligible, but, especially for nonstandard designs, significant loss mechanisms (and, therefore, fluctuation producers) could be overlooked if the complete mechanical configuration is not measured *in situ*.

Dissipation Mechanisms

One of the keys to evaluating mechanical-thermal noise is in understanding the sources of dissipation in the system. In terms of fluctuations, any mechanism that allows energy to escape from the orderly motion of the sensor counts as dissipation. These mechanisms include mechanical damping in the spring and supports, viscous drag, acoustic reradiation, electrical leakage, and magnetic hysteresis.

Since it is often very difficult to separate various damping mechanisms in a device, measurement of the system's Q is a valuable technique for noise assessment. As long as the damping is independent (or nearly so) of frequency, the Q gives the mechanical resistance directly in terms of the resonance frequency and either the mass or stiffness ($Q = \omega_0 m/R = k/\omega_0 R$). Also, the Q is the reciprocal of the loss tangent or the reciprocal of twice the damping factor. Many times, measurements of a vibrating system's dominant mass and Q are simple; the resistance and, therefore, the fluctuating force can be calculated from these measurements.

For capacitive sensors, the very thin gaps that permit low polarization voltage and high capacitance per unit area also lead to squeeze-film damping: the viscous loss associated with squeezing the fluid out between moving surfaces [24-26]. Squeeze-film damping can easily dominate the dissipation mechanisms for gaps of several microns. For two parallel disks of area, S , with average spacing, h_0 , the equivalent mechanical resistance is

$$R_{\text{film}} = 3 \mu S^2 / 2 \pi h_0^3 \quad (20)$$

where μ is the fluid's viscosity (20×10^{-6} kg/m s for air at 20°C ; 10^{-3} kg/m s for water at 20°C). Notice the strong dependence on the spacing. If one disk is perforated, the damping can be reduced considerably [27].

If a moving object is not near another surface (and the Reynold's number is very low as would be expected for acoustic motion), the mechanical resistance is given by Stoke's formula [28, 29]. For a disk of radius, a , moving broadside (a reasonable model for an accelerometer mass or a pressure sensor's diaphragm), Stoke's formula gives

$$R_s = 16 \eta a \quad (21)$$

where η is the fluid's viscosity (20×10^{-6} kg/m s for air at 20°C ; 10^{-3} kg/m s for water at 20°C).

Radiation resistance can be a significant dissipation mechanism above 5 or 10 kHz and, for micromachined sensors with very small diaphragm masses,

radiation mass loading can greatly exceed mechanical mass. The radiation impedance for a simple pressure sensor is approximated closely by [11]

$$Z_M = \rho c \pi a^2 \left[(ka)^2 / 4 + i 0.6 ka \right] \quad (22)$$

where k is the acoustic wave number (ω/c), ρ and c are the density and sound speed of the fluid, and a is the radius of the piston. (The convention $e^{+i\omega t}$ is assumed.) Notice that the equivalent resistance (the real part of Z_M) is a function of frequency; consequently the resulting noise is not white but, instead, increases with frequency. On the other hand, the equivalent radiation mass loading (the imaginary part of Z_M divided by ω) is not a function of frequency.

The radiation impedance for an accelerometer immersed in a fluid is approximately that of an oscillating sphere [30]

$$Z_{MECH} = \rho c \pi a^2 \left[(ka)^4 / 3 + i 2 ka / 3 \right] . \quad (23)$$

For any sensor, the reradiation affects the external surface of the transducer and the expression for this equivalent noise pressure does not contain any of the properties of the transducer. Consequently, this equivalent noise can and usually is included in the ambient sea (or air) noise pressure [31, 32]:

$$\begin{aligned} p_{rad} &= F_{rad} / A = \sqrt{4k_B T R_{rad}} / A \\ &= 2 f \sqrt{k_B T \pi \rho / c} \\ &= 1.8 \times 10^{-4} f \quad [\mu\text{Pa}/\sqrt{\text{Hz}}] \end{aligned} \quad (24)$$

in water. This result also applies to immersed accelerometers if they are neutrally buoyant. The effective noise pressure is well below the SS0-10dB curve over the entire range of 0.1 to 1000 Hz. This noise component dominates ocean ambient noise above 50 or 100 kHz so it is only a concern for very high frequency underwater systems.

(Note: The same result for p_{rad} can be obtained by calculating the pressure that results from giving each normal mode in the ocean an energy of $k_B T/2$. The reradiation component is sometimes mistakenly taken to be the entire thermal noise component in a sensor but this ignores all of the microscopic energy-storage modes in the sensor structure and fill fluid. From the standpoint of thermal excitation, a microscopic (molecular) mode is no less important than a macroscopic mode like an acoustic mode in the ocean.)

A interesting variety of thermal noise is that associated with leaky dielectrics [33]. This dissipation is characterized by a loss tangent ($\tan \delta$) that can be nearly independent of frequency over a wide range of frequencies. The current-voltage relationship for a capacitor with a leaky dielectric is

$$I = i \omega C V \exp(-i\delta) \quad (25)$$

The real part of the equivalent impedance (for small δ) is $\tan\delta/\omega C$ so the open-circuit noise voltage is

$$V_{oc}^2 = 4 k_B T \tan\delta / \omega C \quad (26)$$

The thermal noise associated with this dissipation has a spectrum that is not white but, rather, $1/f$. (Clearly, the loss tangent cannot be independent of frequency all the way down to DC because this would require infinite fluctuation power.) Many capacitive micromachined sensors use air (or vacuum) as the dielectric where the loss tangent is negligible; however, in those cases where a liquid might be used (to resist hydrostatic pressure in a hydrophone, for example), this noise component should be calculated especially since the micromachined sensor is likely to have very small capacitance (V_{oc}^2 is proportional to $1/C$).

Example 4. A fluid-filled capacitive hydrophone has a receiving sensitivity of -185 dB (1V/ μ Pa) and a capacitance of 400 pF. If the loss tangent of the dielectric fluid is 0.01, what is the equivalent noise pressure corresponding to the open-circuit voltage noise due to the leaky dielectric?

NADC-91113-50

From Eq. 26, the open-circuit voltage-squared is $6.4 \times 10^{-16} / f$ volts-squared per hertz. At 1 Hz, this is -132 dB(V). From the receiving sensitivity, the corresponding pressure is 60 dB($1\mu\text{Pa}^2/\text{Hz}$), which is well below the SS0-10dB curve. This noise component increases with decreasing frequency but the ocean ambient also increases (faster) with decreasing frequency.

The following examples illustrate why ignoring thermal noise in *conventionally-sized* underwater sensors has not created a problem:

Example 5. A standard piezoceramic hydrophone (pressure sensor) has the following characteristics: $f_0 = 1600$ Hz, $Q = 5$, $m = 0.4 \times 10^{-3}$ kg, and $S = 3$ cm². If it is to be used from 0.1 to 1000 Hz, will thermal noise be a problem?

Again, the worst case is at 1000 Hz. From Eq. 19, the signal-to-noise ratio at 1000 Hz is 20 000 so thermal noise is not a problem.

Example 6. A conventional geophone can be modeled as a simple accelerometer. If a geophone [23] has $f_0 = 28$ Hz, $m = 2.2$ gm, and a damping factor $\zeta = 0.18$, will thermal noise be a problem?

Here, the worst case is at 10 Hz where $a_n = 5.3 \times 10^{-8}$ m/s². (Use Eq. 8 to calculate Q.) From Eq. 17, the signal-to-noise ratio at 10 Hz is 6. While this is not as large as in the previous example, thermal noise would not be a problem in this case either.

Mechanical thermal noise is often overlooked as limiting noise source because conventionally sized underwater sensors have thermal noise well below the quietest background noise in the ocean. Thermal noise can be a serious issue though for very small sensors as Examples 1 through 3 illustrate. Small physical size should not be the criterion for deciding whether or not to consider mechanical-thermal noise; this noise component should be evaluated for any sensor that is intended for extreme sensitivity. For example, mechanical-thermal noise is routinely considered in the design of gravity-wave detectors [34] even though these detectors are physically very large.

Noise Estimation from Sensor Frequency Response

Sometimes the information available for a sensor is insufficient to directly calculate Q or R. One consequence of equipartition is that the details of damping need not be known. The total thermal energy is fixed by equipartition; the system's frequency response can only redistribute that energy. If a frequency response curve (measured or theoretical) is given for the sensor, this curve can be used to evaluate the mechanical-thermal noise for simple sensors.

In order for this to work, the spectral shape of the signal response of the sensor must be the same as the spectral shape of the output of the sensor due to thermal agitation of the sense element. For the simple accelerometer, the spectral shape of the acceleration response is identical to the shape of the noise response (Eq. 11); for the simple pressure sensor, the shape of the pressure response is identical to the shape of the noise response (Eq. 18). This may not be true for more complicated sensors but, if the behavior is dominated by a single mass-spring system, then the following procedure may be suitable as a first approximation to the noise characteristics.

The spectral density of the noise is generally not constant with frequency because the mechanical spring-mass system shapes the spectrum but the broadband noise is still governed by equipartition so

$$\langle x^2 \rangle = \int_0^{\infty} x^2(f) df = k_B T / k \quad (27)$$

(Note: this is the appropriate starting point if the sensor output is proportional to the *displacement* of the sensor mass; if, as in the case of a moving-coil accelerometer, the output is proportional to the *velocity* of the mass, then $\langle v^2 \rangle$ and Eq. 3 should be used to write the velocity equivalent of Eq. 27.) This expression says that the energy in the mode associated with the mean-square displacement is constant regardless of its spectral distribution.

Figure 6 shows the spectral distribution of the mean-square displacement for three systems with the same k (so the right-hand side of Eq. 27 remains constant), but different resonance frequency or Q . The spectral shape is different in each case but the area under each curve is the same. For example, increasing the Q does not reduce the total noise energy, but it concentrates the energy near the resonance thereby reducing it in the band below resonance.

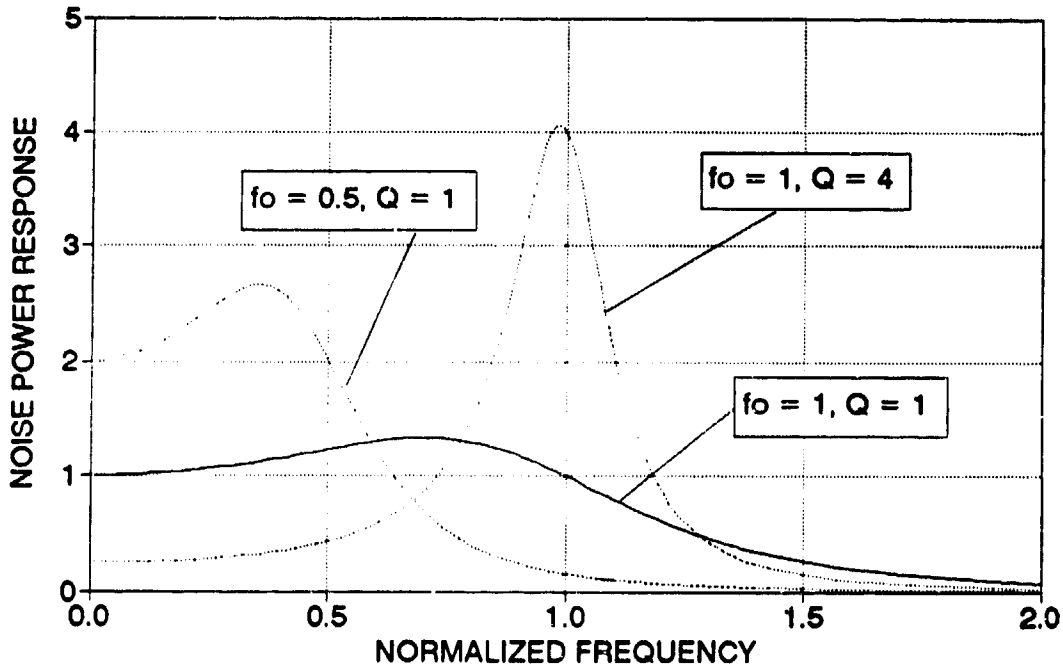


Figure 6. Noise power distribution for three oscillators with the same spring constant but different resonance frequencies and Q 's.

If the given sensor power response function is called $G(f)$ and the displacement noise has the same shape, then $x^2(f) = c_1 G(f)$ and all that is needed is the value of the constant c_1 . This is found directly from Eq. 27: the integral is simply the area, A_f , under the response curve so

$$c_1 = k_B T / k A_f \quad (28)$$

and

$$x^2(f) = G(f) k_B T / k A_f \quad (29)$$

(When the area is calculated, the curve must be expressed in a power-like quantity — displacement squared, pressure squared — and certainly never in dB.) Once the displacement noise is known, the factor relating sense mass displacement to sensor output can be used to calculate the sensor output noise. For a moving-coil sensor whose output is proportional to the velocity of the moving element, the equivalent velocity noise expression is

$$v^2(f) = G(f) k_B T / m A_f \quad (30)$$

Example 7. A pressure sensor with an equivalent spring constant of 10^5 Nt/m has a flat frequency response between 0 and 500 Hz and rolls off rapidly beyond that. Evaluate its mechanical-thermal noise.

The response can be approximated by $G(f) = 1$ from 0 to 500 Hz and $G(f) = 0$ above 500 Hz. The area under the curve is then 500 and Eq. 29 then gives $x = 9 \times 10^{-15}$ m/ $\sqrt{\text{Hz}}$. If the active face of the sensor were 3 mm by 3 mm, then the equivalent noise pressure would be the equivalent noise force, kx , divided by this area. In this case, the noise pressure is $56 \mu\text{Pa}/\sqrt{\text{Hz}}$, which is roughly equal to the SS0-10dB curve at 500 Hz.

Sensors with Feedback

One of the ways of reducing the mechanical-thermal noise is to increase the Q of the sensor. As has been discussed, a high Q can cause dynamic range problems in that out-of-band signals can produce large excursions of the sense mass and these excursions must be accommodated by the mechanical design in order that the in-band signals not be distorted.

There is a means for eliminating this mechanical problem and that is by negative feedback: the output of the sensor is amplified and applied to a force-generating mechanism that opposes the motion of the sense element. If properly done, the feedback force keeps the sense element virtually stationary and the sensor output is taken from the input to the feedback force generator. This is sometimes known as force-balance feedback.

In this way, the mechanical frequency response is made effectively flat and the mechanical dynamic range problem is eliminated. Even if the sensor output without feedback is not linearly related to the sense mass motion (the electron-tunneling sensor is inherently nonlinear), the sensor output with feedback is linear.

These improvements are not, however, free. If the phase response of the feedback loop is not carefully controlled, the intended negative feedback can become positive at some frequencies and the sensor can be driven into self oscillation. Also, negative feedback does not reduce the effects of thermal noise; in fact, the feedback loop adds additional noise. Finally, while the mechanical dynamic range problem is eliminated, the feedback circuitry must have sufficient electrical dynamic range to successfully force-balance the mass motion through the resonance. Fortunately, electrical dynamic range is usually easier to come by than mechanical dynamic range.

The implementation of feedback in the simple accelerometer is shown schematically in Fig. 7.

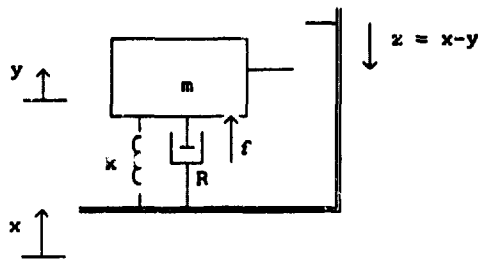


Figure 7. Simple accelerometer with feedback force applied.

The force, f , is applied to oppose the motion of the mass. (Two ways in which the force can be applied are electrostatically or by means of a piezoceramic element.) The control circuit (using frequency domain notation) would look something like the circuit in Fig. 8.

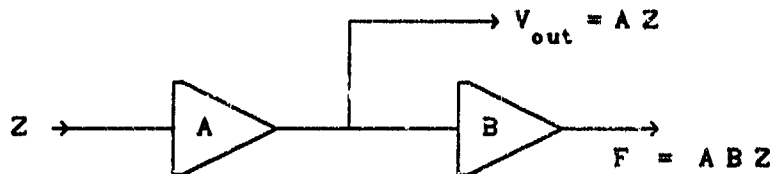


Figure 8. Control circuit for force-balance feedback.

A is the gain of a very high gain displacement-to-voltage conversion stage and B is the transfer constant for the voltage-to-force transducer.

In the frequency domain, the response Z to a case displacement X is

$$Z_s = \omega_m^2 X / \left[\omega_m^2 - i\omega R - (k + AB) \right] \quad (31)$$

which, for very large A (i.e., $AB \gg \omega_m^2$), becomes

$$Z_s \approx \omega_m^2 X / AB \quad (32)$$

Since A is very large, Z_s is kept very small by the feedback force. The actual sensor output is the voltage input to the feedback force transducer. This voltage is

$$V_{out} \approx \omega_m^2 X / B = m a_g / B \quad (33)$$

in terms of the case acceleration, a_g . Notice that the response to signal is flat as long as the frequency is low enough so that $AB \gg \omega_m^2$; the higher the feedback gain, the higher the high-frequency rolloff is. Besides removing the response peak around the resonance, the high frequency rolloff can be delayed by high gain in the feedback loop.

For noise response, the sense mass displacement Z is

$$Z_N \approx F_N / AB \quad (34)$$

and the corresponding voltage output is

$$V_{out} \approx \sqrt{4k_B TR} / B \quad (35)$$

Consequently, the signal-to-noise ratio is obtained by squaring Eqs. 33 and 35 and dividing:

$$\left| \frac{V_s}{V_n} \right|^2 = \frac{a_s^2 m^2}{4k_B TR} = \frac{a_s^2 m Q}{4k_B T \omega_0} \quad (36)$$

which is identical to the expression without feedback given in Eq. 17. So feedback does not improve the sensor's immunity to thermal noise. In fact, components in the feedback circuit will introduce additional noise. Because feedback permits use of high Q , the introduction of additional noise in the feedback loop may be more than offset by the noise reduction from increased Q .

Compound Sensors

The foregoing analyses apply to sensors that are well-represented by a single mass-spring system. While this is adequate for many hydrophones, some designs are more complex. The solution procedure for more complicated systems is more tedious but it is, in principle, identical to the simpler systems.

For example, consider an accelerometer with two mass-spring components. A schematic diagram and the relevant free-body diagrams are shown in Fig. 9.

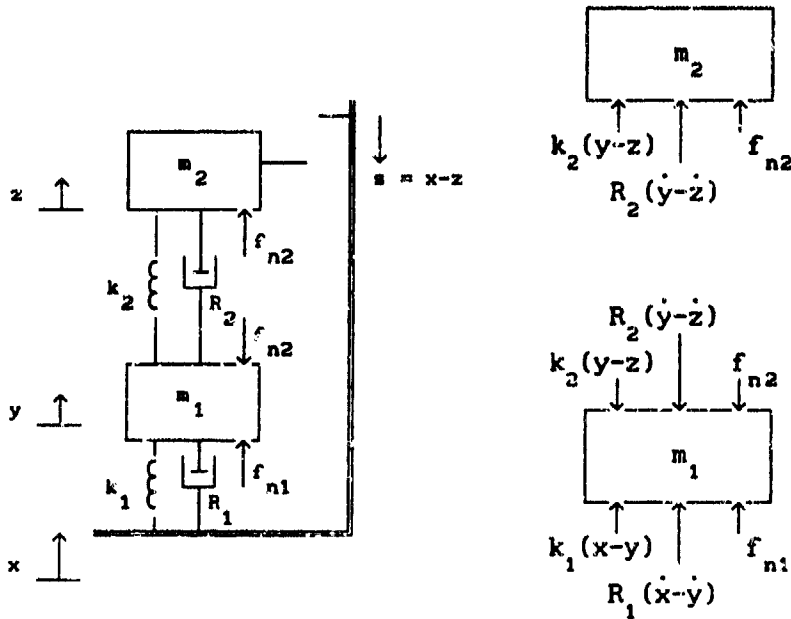


Figure 9. Configuration and free-body diagrams for a compound accelerometer.

As before, the analysis is more conveniently done in the frequency domain. To get the signal response, set F_{n1} and F_{n2} to zero and solve for $S_s (= X - Z)$ as a function of the case displacement X . To get the noise response, set X to zero and set F_{n2} to zero and solve for S_{n1} as a function of F_{n1} ; then set X and F_{n1} to zero and solve for S_{n2} as a function of F_{n2} . Since noise powers add, the total noise is $S_n^2 = S_{n1}^2 + S_{n2}^2$. Also, $F_{n1} = \sqrt{4k_B TR_1}$ and $F_{n2} = \sqrt{4k_B TR_2}$.

In the accelerometer limit ($\omega \ll \omega_1, \omega_2$), the signal response is

$$S_s = -X (\omega/\omega_1)^2 \left[1 + (\omega_1/\omega_2)^2 (1 + k_2/k_1) \right] \quad (37)$$

and the signal-to-noise ratio is

$$\text{SNR} = \frac{a_s^2 m_1 Q_1}{4k_B T \omega_1} \left[\frac{(1 + m_2/m_1 + \omega_1^2/\omega_2^2)^2}{1 + (m_1/m_2)(Q_1/Q_2)(\omega_1/\omega_2)^3} \right] \quad (38)$$

If $m_2 \ll m_1$, $\omega_2 \gg \omega_1$, and the k 's and the Q 's are about equal for the two mass-spring systems, the factors in square brackets are approximately equal to one and the expressions reduce to those of a single mass-spring system.

Complex mechanical devices are, perhaps, best analyzed by first drawing the electrical equivalent circuit and then using a computer-based circuit analysis program to determine the frequency and noise response. This approach is discussed in Appendix B.

Limits of Applicability

Just because a sensor passes the thermal noise test does not mean that it will not have a noise problem. One of the other noise factors discussed in subsequent sections may dominate. However, if it fails the thermal noise evaluation, then the sensor does have a problem.

The noise terms are not really uniformly distributed over all frequencies — that would imply infinite power. More correctly, the factor $k_B T$ should be replaced by [13, 17]

$$\frac{hf}{\exp(hf/k_B T) - 1} \quad (39)$$

where h is Plank's constant (6.6×10^{-34} J s). For $hf \ll k_B T$ this expression reduces to $k_B T$ but above $hf = k_B T$ in frequency, the noise power is reduced. At room temperature, this rolloff occurs above about 10^{13} Hz; so, this is not a concern for typical underwater acoustic sensors.

Some authors [35-37] include the zero-point energy term in Eq. 39, which amounts to an additional $hf/2$. Whether or not this term should be included is the subject of some debate [37] and, since it is not significant below 10^{13} Hz, it is only of academic interest here. While its inclusion does produce the "proper" limit as T goes to zero it also makes Eq. 39 diverge at high frequency. The zero-point energy does put an ultimate limit on optical systems and cryogenically cooled systems [38, 39] but the zero-point energy cannot be extracted from the system [35] and so, from the standpoint of noise power delivered to the observer, need be considered only as a fundamental limit on the observability of a process.

Shot Noise

If a system is in equilibrium, then thermal noise provides a complete description of its internal fluctuations. There are, however, several important non-equilibrium sources of noise [18]: One of these is shot noise.

If a signal is carried by discrete "particles" (electrons or photons, for example) and these particles are emitted randomly, then there will be noise associated with that signal. In the case of an electrical current, the spectral density of the noise component of that current is [40, 41]

$$i_N = \sqrt{2 I e} \quad [\text{amps}/\sqrt{\text{Hz}}] \quad (40)$$

where I is the average current flowing and e is the charge on an electron (1.6×10^{-19} coulombs per electron). This is shot noise.

Photons generated by a laser, charge carriers crossing potential barriers at semiconductor junctions, and electrons emitted from the filament in a vacuum tube are all examples of random emissions that lead to shot noise. On the other hand, the current produced by applying a voltage to a conductor is spatially correlated over large distances and results in very little shot noise [19, 40, 42, 43]. Shot noise results from charge carriers crossing

potential barriers of some sort and the process of jumping the barrier is random.

In a bipolar junction transistor, the charge carriers are randomly injected into the emitter-base and base-collector depletion layers and it is in these layers that the carriers interact with externally applied voltages [18]. These layers are too thin (*i.e.*, the transit times of the carriers are too short) to permit the carriers to reach equilibrium with the "stationary" molecules. Consequently, the noise produced in the external circuits by these junctions is directly related to the randomness of the transit of carriers across the junction rather than being related to thermal vibrations in the semiconductor lattice. This noise is primarily shot noise.

In a field-effect transistor (FET), the carriers interact with the external voltages in a channel that is long enough to allow the carriers to reach thermal equilibrium with the channel. Consequently, the characteristics associated with the random emission into the channel are lost and the noise in a field-effect transistor is primarily thermal noise.

Even if the photon generation by a laser were not random, detection of that light by a photodiode involves random emission of electrons in response to the incident photons, so the photodiode output has shot noise. A typical value for photodiode sensitivity is one microamp output for two microwatts of light input: this value is not arbitrary but is the result of each incoming photon (with a frequency in the visible-light range) forcing a single electron out.

Example 8. Suppose a fiber-optic interferometric accelerometer [44] uses 200 μW of optical power, which produces 100 μA of current out of the photodiode. The mass is 0.54 kg, the resonance frequency is 240 Hz, and the Q is 10. Interferometer sensitivities are often given in terms of radians of phase shift (in the interference fringes) per sensed quantity. In this case, the phase shift per unit displacement of the sense mass is 8500 radians per micrometer of displacement. The sensitivity can be

increased simply by adding more fiber to arms of the interferometer. If the laser noise is 50 μ radians per $\sqrt{\text{Hz}}$, is there any point to increasing the sensitivity?

This sensor has both shot and thermal noise components. Analyze the shot noise first. An interference fringe goes from light to dark so there would be (at most) a 100 μ A current change corresponding to π radians (a half cycle) of fringe shift. The electrical sensitivity is then $100/\pi$ or about 30 μ A/rad. The worst-case shot noise is for an average current of 100 μ A so the shot noise spectral density (Eq. 40) is $i_n = 6 \times 10^{-12} \text{ A}/\sqrt{\text{Hz}}$ and the minimum detectable signal, in terms of fringe shift, is then $\phi_{\min} = i_n / (30 \mu\text{A/rad}) = 0.2 \mu\text{rad}/\sqrt{\text{Hz}}$. This is well below the laser noise so this sensor is not shot-noise limited.

The noise displacement of the sense mass resulting from thermal noise can be calculated from Eq. 13. The displacement noise is $9.3 \times 10^{-16} \text{ m}/\sqrt{\text{Hz}}$. For an optical sensitivity of 8500 rad/ μm , the corresponding phase noise is 8 $\mu\text{rad}/\sqrt{\text{Hz}}$. Although this is greater than the shot noise, the laser noise still dominates. Consequently, the overall sensitivity of this accelerometer could be increased (with more fiber) somewhat.

Example 9. Accelerometers are not sensitive to hydrostatic pressure (that is, until the case implodes!) but a pressure sensor is unless it is somehow compensated for the hydrostatic pressure. Another way of saying this is that the simple pressure sensor responds all the way down to DC pressure. Suppose that an uncompensated fiber-optic pressure sensor has been designed to operate between 100 and 300 meters depth over the frequency range 0.1 to 100 Hz. Suppose that this is not an interferometric sensor but that the variation in light output can be adjusted so that it ranges smoothly from dark to bright over the range of pressure sensed. Evaluate the shot noise performance [45].

Since the sensor is not compensated for hydrostatic pressure variations, it must respond to pressures over the entire hydrostatic range — about 2 MPa here. (Each 100 meters in depth adds about 1 MPa to

the hydrostatic pressure.) If I_{pd} is the maximum current out of the detecting photodiode, then the sensitivity is

$$M = I_{pd} / \Delta P \quad (41)$$

where ΔP is the total required range of pressure to be sensed (2 MPa in this case). I_{pd} is also the current from which to compute the (worst-case) shot noise spectral density i_n from Eq. 40, so the minimum detectable pressure is

$$p_{min} = i_n / M = \Delta P \sqrt{2 e / I_{pd}} \quad (42)$$

The worst case in the band of interest is at 100 Hz where the required p_{min} is $200 \mu\text{Pa}/\sqrt{\text{Hz}}$ so the required photodiode current, I_{pd} , would be 32 amps, which would require an 64 watt laser! In order for this sensor to be a practical underwater sensor, some means would have to be developed to eliminate the DC pressure response.

The shot noise was particularly serious in this last example because the sensor responded to pressure all the way to zero frequency (hydrostatic or DC pressure). A conventional air-backed piezoceramic pressure hydrophone does not respond to DC pressure because leakage currents in the sensor remove the charge produced by very slow straining of the material. Also, the piezoceramic sensor does not modulate a shot-noise producing current, so shot noise is not a consideration.

The spectrum of shot noise is uniformly distributed in frequency ("white") up to rather high frequencies. In order for the shot noise relation to hold, there must be many charge carriers per cycle. There are I/e electrons per second in a current, I , or there are I/ef electrons per cycle at the frequency, f . For a current of 1 nA, there is one electron per cycle at 6×10^9 Hz, so for frequencies well below this, the shot noise spectrum would be white. Increasing the current increases the high-frequency limit.

1/f Noise

Except for a very high frequency cutoff, the fundamental mechanisms of both thermal and shot noise are uniformly distributed in frequency. There is, however, a very commonly occurring noise component whose spectral distribution is not flat but, instead, drops with increasing frequency so that the power distribution is approximately f^{-1} . This sort of behavior is seen in measurements of the base current of transistors, the speed of ocean currents, the flow of sand in an hourglass, the yearly flow of the Nile over the last 2000 years, traffic flow on expressways, sunspot activity, and the loudness of classical music [40, 46, 47].

Unfortunately, there is no simple physical model capable of explaining this noise component as there is in the case of thermal or shot noise [48, 49]. The fact that this 1/f distribution of power occurs so often in so many vastly different settings suggests that the underlying explanation should not depend on the specific details of any single physical process. In addition, the 1/f portion of the spectral distribution can extend over many decades so the time scales required to explain this behavior must range from milliseconds to hours or even days in some instances [47].

The distribution is not precisely f^{-1} either. Observations of different processes show that the exponent can range [49] from -0.8 to -1.4. Furthermore, when the exponent is -1 or more negative, some low-frequency cutoff must be present or there would be infinite power in the spectrum [33, 48, 49].

One attempt to model the spectral shape of this noise component relies on a distribution of relaxation times for the process [49]. Roughly speaking, relaxation time is the time it takes a system to return to "normal" after being disturbed. If the system reverts to its undisturbed state immediately (i.e., it has no "memory"), then the associated power spectrum is independent of frequency. If the system has one characteristic relaxation time, τ , then

the spectral shape is

$$w(f) = A \tau / [1 + (\omega\tau)^2] \quad (43)$$

where A is an arbitrary constant. This spectrum varies as $1/f^2$ for $\omega\tau \gg 1$ (or $f \gg 1/2\pi\tau$).

If, for some reason, a system has a distribution of relaxation times and the probability distribution of those τ 's has just the right shape, then a $1/f$ spectrum results. For example, if the relaxation time is controlled by some sort of energy, E, τ is likely to be exponentially related to that energy ($\tau = \tau_0 \exp(E/k_B T)$); if the probability distribution of the energy is uniform over some range of τ , then the spectrum will have $1/f$ slope over the equivalent frequency range. A reasonable physical model for $1/f$ noise in semiconductors has been developed based on such a distribution of relaxation times where the relaxation processes are connected with trapping and release of the charge carriers ("generation-recombination" noise) [41, 49]. This approach has not been so successful in describing, for example, $1/f$ noise in metallic conductors.

In electrical devices, the $1/f$ noise is proportional to the current passing through the device. Some authors have suggested that the noise results from random fluctuations in resistance that are sensed by the current rather than from fluctuations caused by the current [33, 48, 49]. This conclusion contradicts the notion that $1/f$ noise is a non-equilibrium phenomenon; some external source of energy would be required to keep the resistor from equilibrium and the most likely suspect is the current. In some materials, the noise is proportional to the volume of material, but the noise is often sensitive to surface conditions as well.

Any component that carries current is a potential source of $1/f$ noise [18] in addition to thermal noise [37]. Carbon resistors produce much more $1/f$ noise than wirewound resistors and so should be avoided (in favor of either wirewound or metal-film resistors) in low-noise preamplifiers. Contact resistance — bad solder joints, terminal lugs screwed to aluminum frames —

can contribute significant amounts of $1/f$ noise. Poor selection of capacitor types for coupling or bypass capacitors (especially through leakage currents) can contribute also: electrolytic capacitors are particularly poor; ceramic capacitors are moderately poor; polyester are acceptable; and teflon, polystyrene, and polypropylene capacitors are excellent. Polarized capacitors should be avoided where possible. For applications requiring large capacitance, tantalum capacitors are acceptable. Any polarized capacitor must be protected against reverse DC bias, which may occur during power-on transients, because they can emit noise pulses up to several hours afterward [50].

Because there is no simple predictive technique to estimate the magnitude of $1/f$ noise, its effects must generally be measured. Fortunately, manufacturers often provide sufficient information about transistors and amplifier chips to allow estimation of noise (of all sources including $1/f$). The next section summarizes how to use this information. Before turning to that topic though, it is worth pointing out that $1/f$ noise is not only a low frequency problem. Oscillators must be nonlinear in order for their amplitude to be stable and this nonlinearity coupled with $1/f$ noise results in sidebands on the oscillator output [18].

It is also possible that $1/f$ noise is not limited to the electrical part of a sensor. Mechanical parts in the sensor assembly may also contribute $1/f$ noise according to one study of condenser microphones [51-53]. In this case, the energy required to keep the system from equilibrium was likely to have been the polarizing voltage.

An effective way of avoiding the effects of $1/f$ noise in very-low-frequency measurement systems is to arrange the signal to modulate a high-frequency reference signal. For example, a capacitive sensor can be used in an AC bridge circuit. If the sensor is in one leg of the bridge and a reference capacitor is in the other, then the output is a differential signal: oscillator noise effectively cancels out since its signal flows through both branches.

Even better if the sensor itself can be designed with a "push-pull" output. A capacitive accelerometer could be built with the moving plate suspended between two stationary plates. The two capacitors so formed would be used in the bridge circuit, one in each leg.

Another approach is to use an inductor to form a tuned circuit that is driven electrically at its resonance. The phase shift resulting from capacitance changes is directly proportional to the electrical Q (see Eq. 9). This approach does not by itself remove the oscillator noise but a bridge circuit can be constructed in which each leg of the bridge contains a tuned circuit [43].

Amplifier Noise

Once the sensing element itself has been designed for adequate noise performance, it is usually necessary to amplify the resulting signal to a useable level. While electrical noise calculations are much more familiar than mechanical noise calculations, it is worth summarizing the principles here because a poor preamplifier can negate the noise performance of a quiet sensor.

The safest way to analyze the noise performance of a preamplifier circuit connected to a sensor is to calculate the signal-to-noise ratio directly from the manufacturer's data (or measurements) for the equivalent input noise voltage and current for the transistors or chips [18, 40, 54]. This is the procedure that will be outlined below, but some more common but less useful definitions will be mentioned first in order to warn of some dangers and to make connections between alternate expressions of noise performance.

One of the most commonly quoted noise measures is noise figure. Noise figure is ten times the common logarithm of the noise factor; noise factor for a particular device is the ratio of the signal-to-noise power at the input of

the device to the signal-to-noise power at the output of the device:

$$\begin{aligned} \text{noise factor} &= nf = \text{SNR}_{\text{INPUT}} / \text{SNR}_{\text{OUTPUT}} \\ \text{noise figure} &= NF = 10 \log (nf) \end{aligned} \tag{44}$$

Defined this way, noise factor is always greater than one (and noise figure is always positive) and is a measure of the degradation in signal-to-noise ratio caused by the device.

This sounds like a good approach but, in practice, device manufacturers often quote only the optimum noise figure. Noise figure is a strong function of source resistance, so if the source resistance is not given for that noise figure or the stated source resistance is not close to the actual source resistance used, the noise figure is of little value.

Equivalent input noise sources

Of far more value are the manufacturer's specifications for equivalent input voltage and current noise for the device. By convention, these values are equivalent values *at the input to the device* and so are added to the source noise contributions (thermal, shot, 1/f). The output levels can be found simply by multiplying by the device gain but the signal-to-noise ratio remains the same. In effect, the real device has been replaced by a noise-free amplifier and voltage and current noise generators as in Fig. 10.

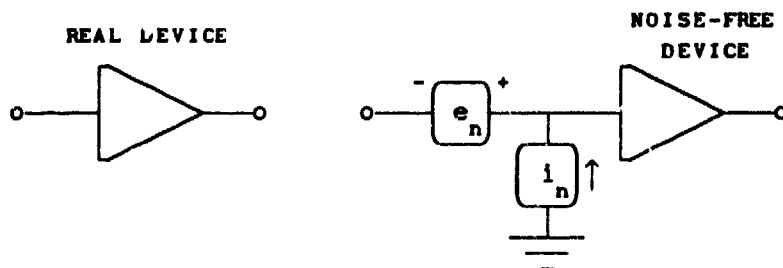


Figure 10. Input noise current and voltage generators.

Because the noise voltage and current are given as the equivalent *input* values, the noise figure can be determined from the input noise alone (the ratio of the input signal to the input signal is one!). If the device were truly noise-free (i_n and e_n equal to zero), then the input noise voltage squared would be $4k_B TR_s$ from the source resistance, R_s . In terms of the noise figure, the actual input noise for the real device would then be

$$e^2 = (4k_B TR_s) nf \quad (45)$$

$$\text{or } (dB/V^2)_{\text{input noise}} = 10 \log (4k_B TR_s) + NF$$

This can be misleading, though, because the input noise may not be entirely due to the obvious input circuit resistance. The input noise also includes the mechanical thermal noise of the sensor and, maybe, shot noise and 1/f noise. Of course, an equivalent source resistance could be derived to include all these effects but this is an awkward approach. Again, the best approach is to calculate the equivalent input noise directly and either forget about noise figure altogether or calculate the noise figure directly from the equivalent input noise.

If the source noise can be represented by an equivalent resistance, R_s , then the amplifier can be analyzed using the model of Fig. 11.

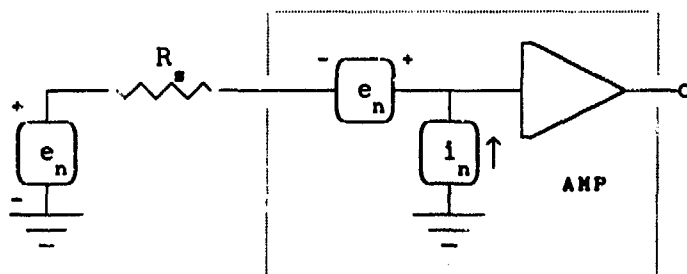


Figure 11. Model for noise analysis of amplifier.

(Note: if the source impedance is complex, take the real part for R_s for those terms representing generation of thermal noise — $4k_B TR$ terms — but use the magnitude of the source impedance for those terms representing voltages

generated by current flowing through the source impedance — $i_n R$ terms, for example.) The equivalent input noise voltage and current [40, 55-57] for several low-noise op amps and one low-noise preamp (LM381) are shown in Figures 12 and 13.

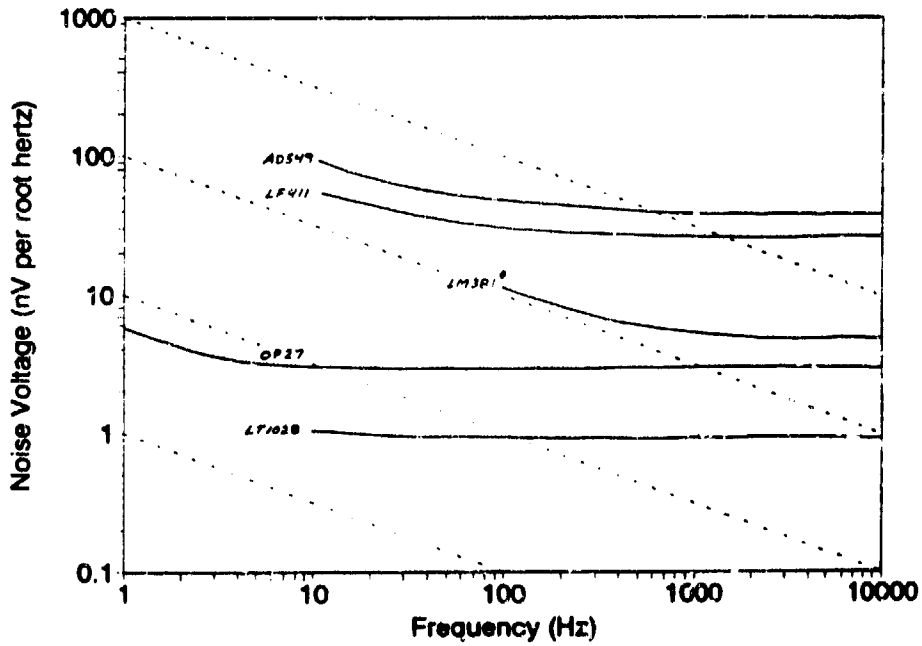


Figure 12. Input voltage noise for several integrated circuits. Dashed lines indicate slope corresponding to $1/f$ noise.

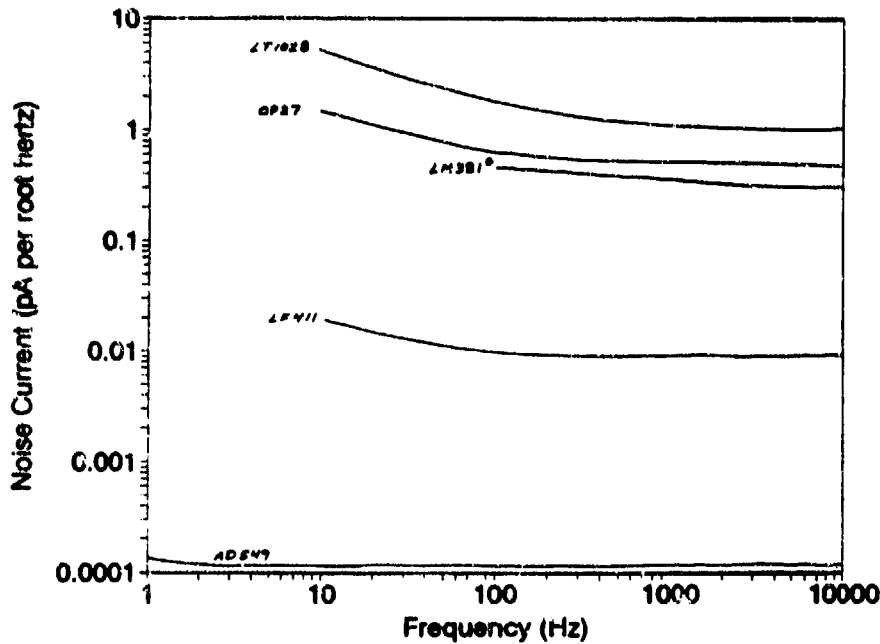


Figure 13. Input current noise for several integrated circuits.

For preamplifier chips and transistors without feedback, the equivalent input noise voltage resulting from the amplifier is

$$e^2 = e_n^2 + (i_n R_s)^2 \quad (46)$$

(Sometimes it is more convenient to calculate the amplifier's input noise current

$$i^2 = (e_n/R_s)^2 + i_n^2 \quad (47)$$

If R_s represents the entire noise contribution of the source, then the total input noise voltage is e^2 from Eq. 46 plus $4k_B T R_s$. This total noise voltage as a function of source resistance is shown in Figure 14 for the devices of Figures 12 and 13.

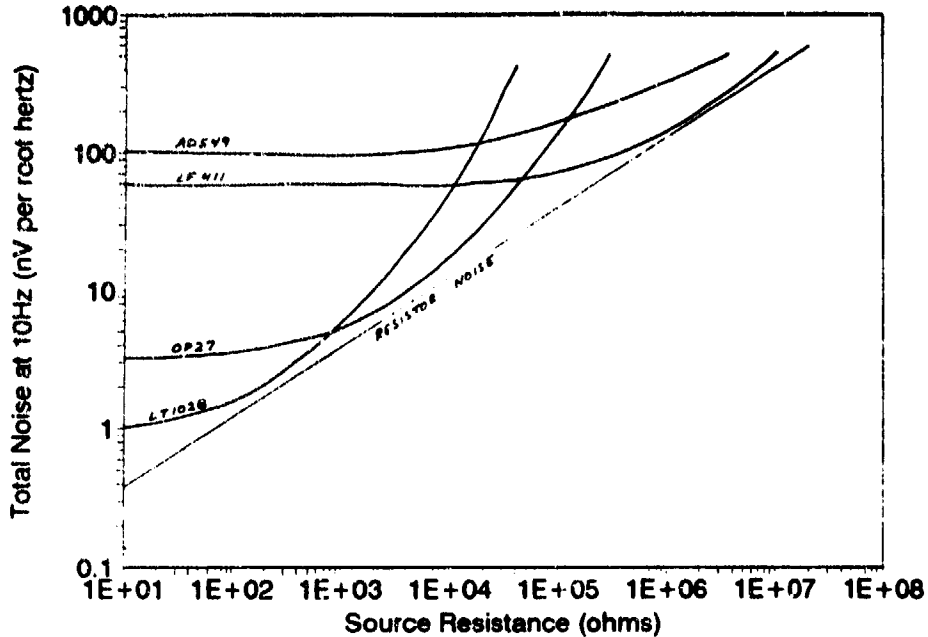


Figure 14. Total input voltage noise as a function of source resistance.

Notice that, in each case, there is an optimum source resistance that results in the smallest noise excess over source resistor noise. Notice also that this optimum resistance is substantially different from device to device. For example, the LT1028 is particularly good for source resistances between 100 and 1000 ohms while the LF411 is good for source resistances between 1 and 10 megohms. For best noise performance, it is not enough to select a low-noise chip; it is also necessary to match the chip to the source impedance.

Operational amplifiers with feedback

The curves in Figure 14 represent the noise performance for the op amps without feedback. This is not realistic since op amps are almost always used with feedback and the feedback circuits add additional noise (both from thermal noise in the feedback resistors and interaction of the amplifier i_n and e_n with the feedback resistors). For the noninverting feedback

configuration (see Appendix C) shown in Fig. 15,

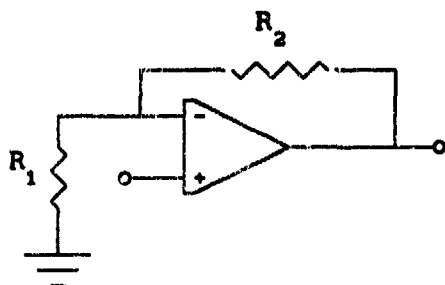


Figure 15. Noninverting configuration for an operational amplifier.

the voltage gain is $G = 1 + R_2/R_1$ and the total input noise voltage (including source resistor noise) is

$$e^2 = e_n^2 + 4k_B T(R_s + R_p) + i_n^2(R_s + R_p)^2 \quad (48)$$

where R_p is the parallel combination of R_1 and R_2 : $R_p = R_1 R_2 / (R_1 + R_2)$.

For the inverting configuration of Fig. 16,

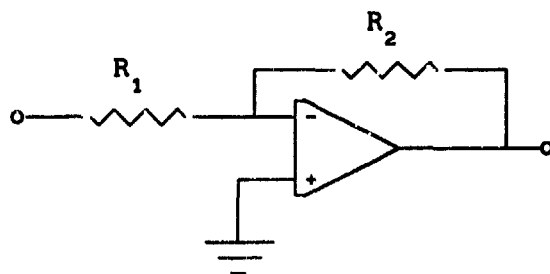


Figure 16. Operational amplifier in inverting configuration.

the voltage gain $G = R_2/R_1$ and the total input noise voltage is

$$e^2 = (1 + R_a/R_2)^2 e_n^2 + 4k_B T R_a + 4k_B T R_2 (R_a/R_2)^2 + i_n^2 R_a^2 \quad (49)$$

where R_a is the sum of R_s and R_1 . A more complete discussion of noise analysis of op amps with feedback and JFET amplifiers is in Appendix C.

By comparing Eqs. 48 and 49 to Eq. 46, it is obvious that feedback increases the amplifier noise contribution. Once the amplifier configuration has been chosen, either Eq. 47 or 48 can be used to calculate the input noise to which must be added any sensor noise component not included in the source resistance R_s . If the sensor noise component is an equivalent current noise, the amplifier noise may be more conveniently expressed as a current: $i^2 = e^2/R_s^2$. In any case, the proper R_s may also include mechanical resistance. The best way to insure that all components are accounted for is to draw the complete electro-mechanical equivalent circuit as described in Appendix D.

(Note: Some low-noise preamplifier chips, such as the LM381 shown in Figures 12-14, have optional differential inputs. If the differential inputs are used, the e_n^2 value for the chip must be doubled (i_n^2 stays the same).)

Example 10. A non-traditional way of sensing the displacement of the sense mass in an accelerometer is by electron tunneling. If a probe is placed very close (10^{-9} to 10^{-10} meters) to a conducting surface and a small voltage is applied from the conducting surface to the probe, a current flows because of wave-like tunneling of electrons across the gap [9, 58]. The actual mechanism of current generation is unimportant here; the important detail is that a current is generated that is proportional to displacement. (The fact that the proportionality is not linear will be ignored.)

Consider an electron-tunneling accelerometer with $m = 25 \times 10^{-6}$ kg, a resonance frequency of 200 Hz and a Q of 200. The change in tunneling current with a change in displacement is 7 amps per meter and the average tunneling current is 1 nanoamp with an applied voltage across the gap of 100 mV. The preamplifier is an inverting op amp with $R_1 = 0$ and $R_2 = 10^7$ ohms. (In this configuration, the op amp acts as a current-to-voltage convertor with an output voltage equal to 10^7 times the input current.) Evaluate the noise performance and select a suitable op amp.

Since this is a current-producing sensor, it is convenient to express all noise components in equivalent currents. The mechanical-

thermal noise displacement is given by Eq. 13, and, when multiplied by the displacement-to-current factor of 7 A/m, the resulting noise current is $2.8 \times 10^{-13} \text{ A}/\sqrt{\text{Hz}}$. The shot-noise current from Eq. 39 is $1.8 \times 10^{-14} \text{ A}/\sqrt{\text{Hz}}$. The tunneling gap has an equivalent resistance equal to the bias voltage (100 mV) divided by the tunneling current (1 nA) or 10^8 ohms; however, this contributes no noise because tunneling is not an equilibrium process: there is no mechanism that can bring the tunneling waves into equilibrium as they transit the gap. Without considering the preamplifier contribution then, this device is limited by mechanical-thermal noise. (The mechanical-thermal contribution is slightly larger than the equivalent SSO-10dB value at 10 Hz but that problem will be ignored in this example.)

The preamplifier noise can be determined from Eq. 49 divided by the source resistance squared (to get i^2) and with $R_1 = 0$:

$$i^2 = i_n^2 + 4k_B T/R_2 + e_n^2 (1 + R_s/R_2)^2 / R_s^2 \tag{50}$$

The first and third terms on the right-hand side reflect the impact of the amplifier current and voltage noise components. The second term results from thermal noise in the feedback resistor and the third term includes the effects of the amplifier voltage noise on the feedback resistor.

In order to illustrate the selection problem with op amps, three types will be considered: two expensive chips — LT1028 and AD549, and one cheap chip — the LF411. The equivalent noise voltage and current for each chip can be estimated from Figures 12 and 13. At 10 Hz, the values are given in Table II.

Table II. 10 Hz noise values for LT1028, AD549, and LF411.

	LT1028	AD549	LF411
e_n [v/ $\sqrt{\text{Hz}}$]	1×10^{-9}	1×10^{-7}	6×10^{-8}
i_n [A/ $\sqrt{\text{Hz}}$]	5×10^{-12}	1×10^{-16}	2×10^{-14}

NADC-91113-50

Table III summarizes the individual current noise components (in amps^2/Hz so that they can be added directly) for the entire system with each of the three choices of op amp. The terms on the right-hand side of Eq. 50 have been named *amplifier current*, *feedback thermal*, and *amplifier voltage* in order of their appearance in that equation.

Table III. Current noise components for sensor/amplifier system.

	LT1028	AD549	LF411
MECHANICAL THERMAL	7.8×10^{-26}	7.8×10^{-26}	7.8×10^{-26}
SHOT NOISE	3.2×10^{-28}	3.2×10^{-28}	3.2×10^{-28}
FEEDBACK THERMAL	1.6×10^{-27}	1.6×10^{-27}	1.6×10^{-27}
AMPLIFIER VOLTAGE	1.2×10^{-32}	1.2×10^{-28}	4.4×10^{-29}
AMPLIFIER CURRENT	2.5×10^{-23}	1.0×10^{-32}	4.0×10^{-28}

For each op amp, the dominant noise component is boxed. Clearly, the expensive LT1028 would be an extremely poor choice since its noise component is much higher than the intrinsic sensor noise. While the LT1028 does have exceptionally low *voltage* noise, its *current* noise is quite high. Since the source resistance is very high in this application, it is necessary to select a chip with low current noise. (The LT1028 would be excellent for applications with very low source resistance.) Both the AD549 and the LF411 would perform well since the sensor noise dominates in both cases but the LF411 is considerably cheaper.

This analysis has been done for 10 Hz, which is the worst-case frequency for designing to the SS0-10dB curve for the simple accelerometer alone. The preamplifier introduces $1/f$ noise, however, so the lowest frequency of interest should also be examined. If, for example, the system is intended to be used down to 0.1 Hz, the amplifier voltage and current noise would be considerably higher. If the manufacturer does not supply equivalent noise values at a low enough frequency, the values can be estimated by extrapolating the given values by $1/f$ (in power). The voltage-squared (or current-squared) noise would be 100 times greater at 0.1 Hz than at 10 Hz. This would increase the values in the last two

lines of the above table by a factor of 100. The LF411 and the AD549 systems would still be adequate.

General Considerations for Preamplifiers [18, 40, 50, 54]

(1) The first stage of amplification usually dominates the noise performance of the electronics. It should be a simple preamplifier that passes the frequency range of interest. Mixers, complex filters and detectors should be saved for later stages.

(2) Don't select an amplifier by noise figure alone. Do the complete analysis as in the previous example and account for the actual source resistance.

(3) Don't add a resistor in series with a source to more closely match the optimum source resistance for a particular amplifier. This may make the noise figure of the amplifier alone lower but it will add more than enough additional thermal noise to compensate.

(4) With op amps, don't forget to include the feedback components in the noise calculations. (Use Eq. 48 or 49, not Eq. 46.)

(5) If the manufacturer's specifications on e_n and i_n don't go low enough in frequency, estimate the appropriate values by extrapolating e_n^2 and i_n^2 as $1/f$. (Do this even if the manufacturer's curve shows a constant value with no low-frequency increase; the $1/f$ breakpoint in the curve is probably just below the given portion.) Of course, don't try to extrapolate beyond the passband of the device.

(6) For systems that require very low noise electronics, better performance can be obtained with a discrete (FET or bipolar transistor) input stage added to an op amp. Here, a JFET would be selected for a high-impedance source, while a bipolar transistor would be selected for a low-impedance

source. MOSFETs are not used for low frequency applications because they have large $1/f$ noise components.

Summary

As the preceding examples illustrate, mechanical-thermal noise can have observable consequences in micromachined sensors. The gross effects can be estimated easily either through Nyquist's Relation or the Equipartition Theorem. Frequently, this estimate is sufficient to determine if there is thermal noise problem. Of course, just because a sensor passes the thermal noise test does not mean that it will not have a noise problem. There are many other sources of noise in an electromechanical transducer system; however, if the sensor fails the thermal noise evaluation, then it does have a problem.

If the sensor can be approximated as a simple pressure sensor or a simple accelerometer, then an estimate for the sensor noise can be made from the sensor Q , from a calculation of the dominant damping mechanism, or from a measured or calculated frequency response. Many times this simple estimate will be sufficient. If not, then a more detailed mechanical analysis or a complete electromechanical equivalent circuit may be required. The effects of the sensor preamplifier can be included if the complete circuit is drawn.

In short, when a high-sensitivity sensor is being designed, an analysis of mechanical-thermal noise should be included at an early stage to avoid being trapped with an unacceptably high noise floor.

Appendix A. Derivation of Nyquist's Relation

Nyquist's relation gives the connection between the spectral density of the fluctuations of a system in thermal equilibrium and the dissipation of that system. Since this relation comes from equilibrium thermodynamics, the result is independent of the physical model used. The following derivation is done for a damped mass-spring oscillator [59-61] but it can be done just as well for a damped inductor-capacitor oscillator [17, 19].

As discussed for the simple pressure sensor, the displacement response, Z , for a damped harmonic oscillator to which an arbitrary force, F , is applied is given by Eq. 13 rewritten here

$$|Z| = F / k \sqrt{(1-\Omega^2)^2 + \Omega^2/Q^2} \quad (\text{A-1})$$

where $\Omega = \omega/\omega_0$.

From equipartition, Eq. 2, $k\langle z^2 \rangle = k_B T$. The quantity $\langle z^2 \rangle$ is equal to the integral of $|Z|^2$ over all frequencies so the equipartition expression can be written

$$k \frac{F_n^2}{k^2} \int_0^\infty \frac{df}{(1-\Omega^2)^2 + \Omega^2/Q^2} = k_B T \quad (\text{A-2})$$

where F_n is the noise driving force, which is assumed to be uniformly distributed over all frequencies. Changing the integration variable from f to Ω yields

$$\frac{F_n^2 \omega_0}{2\pi k} \int_0^\infty \frac{d\Omega}{(1-\Omega^2)^2 + \Omega^2/Q^2} = k_B T \quad (\text{A-3})$$

The denominator of the integral is quadratic in Ω^2 and so can be factored. Then the integral can be solved by complex contour integration but it also

appears in Gradshteyn and Ryzhik [62, Eq. 3.264.2] where its value is found to be $\pi Q/2$. Consequently,

$$\frac{F_n^2 \omega_0}{2\pi k} \frac{\pi Q}{2} = \frac{F_n^2 \omega_0}{4k} \frac{k}{\omega_0 R} = k_B T \quad (\text{A-4})$$

or

$$F_n = \sqrt{4k_B T R} \quad [\text{force}/\sqrt{\text{Hz}}] \quad (\text{A-5})$$

which applies even if R is a function of frequency [16].

As mentioned at the beginning of this Appendix, the same result can be obtained by analyzing a variety of different physical models. Alternative systems leading to the Nyquist relation, Eqn. A-5, are

- (1) A spring-damper system acting on an object with negligible mass [36, 63]. (For example, Langevin's method.)
- (2) A transmission line with matched resistive terminations [21, 43, 64]. This is the device used by Nyquist to obtain the electrical form of his relation (for "Johnson" noise).
- (3) Fermi-Dirac conduction electrons in a metal [17, 37].
- (4) Equilibrium between a small surface and an infinite volume of fluid [32, 65]. This is one of the most interesting examples because the problem can be solved in two ways. The spectral density of the pressure fluctuations can be derived by the acoustic analog of blackbody radiation (as is done for the Rayleigh-Jeans Law) where the surface is assumed to be inside a volume, the frequency distribution for the normal modes in the volume is obtained, the modes are each given their thermal equipartition energy, and the volume is allowed to increase indefinitely. The result is [31]

$$dp^2 = (\rho' \pi k_B T / c) f^2 df \quad (\text{A-6})$$

The Nyquist relation

$$dF^2 = S^2 dp^2 = 4k_B TR df \quad (A-7)$$

where S is the surface element area, implies that the associated resistance is

$$R = \rho \pi S^2 f^2 / c \quad (A-8)$$

From strictly hydrodynamic considerations, the radiation resistance can be calculated for a surface element in an infinite fluid volume and the result is identical to Eq. A-8.

Appendix B. Equivalent-Circuit Modeling with SPICE

Noise analysis can be performed on complicated mechanical systems easily by using a computer simulation of the equivalent electrical circuit. This appendix summarizes the use of one of the popular software tools — SPICE — to do these analyses [66].

The first step is to select an appropriate analogy between electrical quantities and mechanical quantities [65]. For an entirely mechanical system the choice between the impedance or the mobility analog is mostly one of preference. If, however, it is desired to analyze a mechanical transducer with its associated electronics, the natural association of pressure with voltage in a piezoelectric or capacitive sensor favors the impedance analog, while the moving-coil sensor favors the mobility analog. The impedance analog will be used here; relations for the mobility analog can be written similarly.

The impedance analog is as follows:

$$\begin{array}{l} \text{velocity, } v \longleftrightarrow \text{current, } i \\ \text{force, } F \longleftrightarrow \text{voltage, } e \end{array}$$

$$\text{mass: } F = m \frac{dv}{dt} \longleftrightarrow e = L \frac{di}{dt} \quad (\text{B-1})$$

(where v is velocity in inertial frame)

$$\text{spring: } F = k \int v \, dt \longleftrightarrow e = \frac{1}{C} \int i \, dt \quad (\text{B-2})$$

(where v is the velocity *difference* between the ends)

$$\text{damper: } F = R v \longleftrightarrow e = R i \quad (\text{B-3})$$

(where v is the velocity *difference* between the ends)

From these relations it is clear that inductance, L , is the analog of mass, m ; the inverse of capacitance, $1/C$, is the analog of stiffness, k ; and the mechanical resistance, R , is the analog of electrical resistance, R .

The key to the impedance analogy lies in the distinction between the relevant velocity for a mass and the relevant velocity for either a spring or a damper. This distinction is illustrated in Fig. B-1 (mechanical symbol on left, electrical symbol with appropriate "current" on right).

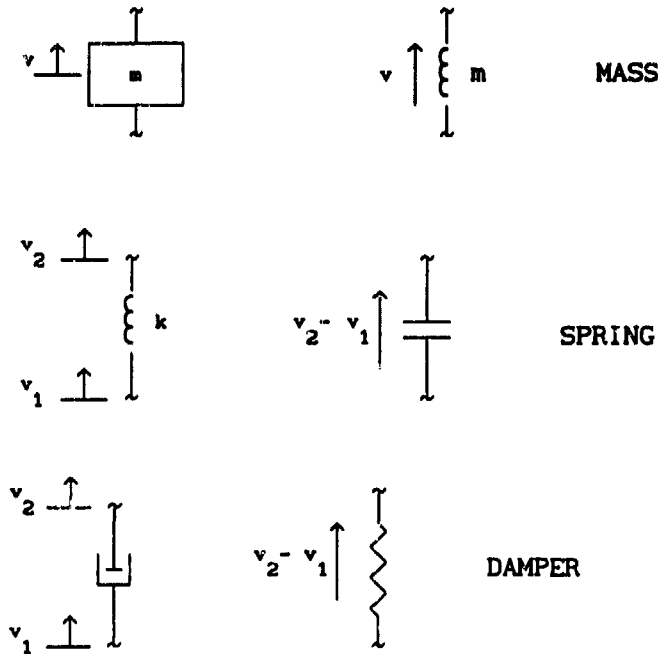


Figure B-1. Electromechanical impedance analogy.

When drawing the electrical circuit, split the current as required to keep the appropriate velocity or velocity difference on the objects. Figure B-2 illustrates this procedure for a simple example.

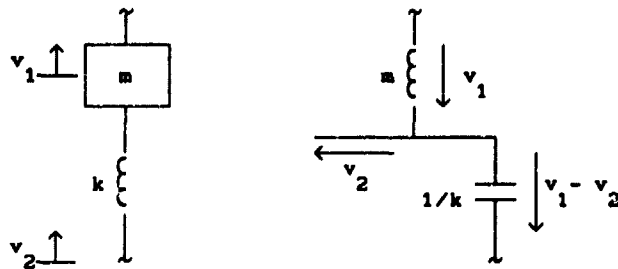


Figure B-2. Construction of impedance analogy and creation of proper branch currents (velocities).

In SPICE, voltage and current (corresponding to force and velocity, respectively) can be monitored easily. When acceleration and displacement must be measured, a small subterfuge is required. To measure acceleration, insert a small inductor, m_0 , and measure the voltage (force) across it. Since $F = m_0 a$, the acceleration at that point is equal to F/m_0 . Obviously the inserted inductor must be small with respect to the other components so as not to influence the circuit behavior.

To measure displacement, insert a small capacitor, $1/k_0$, and measure the voltage (force) across it. The force $F = k_0 x$ so the displacement is equal to F/k_0 . If the circuit values can be arranged so that m_0 and k_0 can be set to one, then the acceleration and displacement can be read directly from the voltage across the probe component.

There is, however, an unfortunate problem with SPICE: all nodes must have a DC path to ground. Insertion of the displacement probing capacitor will often isolate a node from ground. To re-establish DC contact with ground, add a very large inductor in parallel with the probe capacitor (see Fig. B-3).

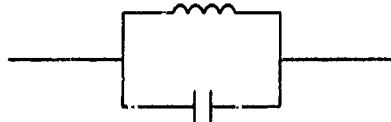


Figure B-3. Use of inductor to provide DC path around capacitor.

Don't use a parallel resistor because that may upset the noise calculation. Also, don't use a small test resistor to measure velocity (current) as this can also upset the noise calculation. To measure velocity, insert an independent voltage source with zero amplitude. SPICE allows the syntax `I(VTEST)` to display the current flowing through the source, `VTEST`.

The total voltage noise is calculated using the `.NOISE` statement. Unfortunately, there is no convenient way to calculate the total current noise directly.

Voltage and current sources in SPICE are used to drive the mechanical system. Pressure is force divided by area (if it is uniform on the transducer face) so a voltage source with an amplitude equal to the desired pressure times area represents the driving pressure. A velocity driver is directly represented by a current source. There is no acceleration (or displacement) source so a velocity source should be used with a series-connected probe inductor (or capacitor) to measure the acceleration (or displacement) drive level.

Before considering some examples of electrical analogs of mechanical devices, the acoustic analogy should be mentioned since some transducers are more easily represented by acoustic lumped parameters rather than mechanical lumped parameters [11]. In the acoustic analogy, current is the analog of volume velocity and voltage is the analog of pressure. Volume velocity, q , is the total volume flow rate through some reference surface and is defined for a vector velocity field, v ,

$$q = \int_{\text{area}} v \cdot dS \quad (\text{B-4})$$

where dS is the differential surface-area element expressed as a vector normal to the surface. Normally, the acoustic analogy is only used if the fluid velocity can be considered to be constant over and normal to the area in question. In this case, the volume velocity is simply $q = vS$ where S is the area. The acoustic analogy is used for devices in which fluid flow is a significant property.

Acoustic impedance is defined as pressure divided by volume velocity and is equal to the mechanical impedance (force divided by velocity) divided by the area squared. Therefore, mechanical elements are represented as follows:

$$\begin{aligned} \text{mass} &\longrightarrow \text{inductor with } L = m/S^2 \\ R_{\text{mech}} &\longrightarrow \text{resistor with } R = R_{\text{mech}}/S^2 \\ \text{stiffness} &\longrightarrow \text{capacitor with } 1/C = k/S^2 \end{aligned}$$

In fluid-filled systems, stiffness elements are often volumes of fluid. For gases, these volumes are represented as [11]

volume \longrightarrow capacitor with $C = V/\gamma p_0$

where V is the volume, γ is the ratio of specific heats (1.4 for air), and p_0 is the ambient pressure. For liquids, replace γp_0 with the bulk modulus,

B. The principles for equivalent circuit construction for acoustic analogs are similar to those for mechanical impedance analogs.

Example B-1. Simple Pressure Sensor. The mechanical-impedance equivalent circuit is shown in Fig. B-4.

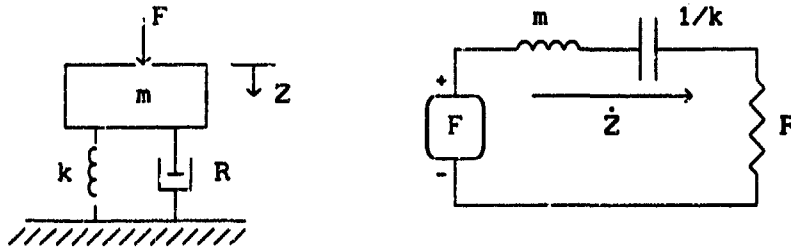


Figure B-4. Equivalent circuit for simple pressure sensor.

and the electrical equivalent circuit with a displacement probe to measure Z (and numbered nodes) is shown in Fig. B-5.

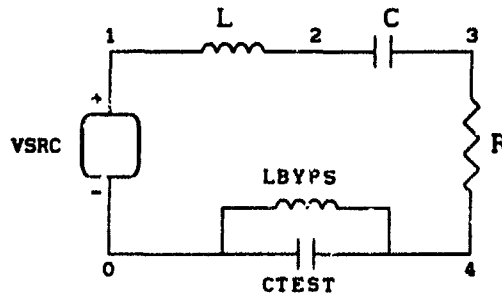


Figure B-5. SPICE equivalent circuit for pressure sensor.

To analyze a specific case, the actual mechanical component values can be used and CTEST can be selected so that $CTEST \gg C$. In this

NADC-91113-50

illustration, however, the values will all be normalized as follows:

- (1) Set CTEST = 1 so that the voltage V(4,0) is directly equal to the displacement, z.
- (2) Pick C << CTEST (e.g., 1E-5)
- (3) Pick L so that the resonant frequency, f_0 , is one. ($\omega_0^2 = 1/LC$ so L = 2533.03 for this example.)
- (4) Pick R to set Q: $Q = \omega_0 L/R$. For Q = 10 in this example, R = 1591.55.

AC analysis gives the sensor output displacement for a constant pressure input; NOISE analysis gives the thermal noise output resulting from R. The following input file for SPICE performs these analyses on this circuit:

```

SIMPLE PRESSURE SENSOR
VSRC  1  0  AC  1  0

L      1  2  2533.03
C      2  3  1E-5
R      3  4  1591.55

CTEST  0  4  1
LTEST  0  4  1E12

.AC DEC 10 0.01 100
.NOISE V(4,0) VSRC 20

.PRINT AC VM(0,4)
.PRINT NOISE ONOISE(M)

.END

```

(A SPICE manual should be consulted for a detailed explanation of these statements [66]).

For a frequency well below the resonance (e.g., $f = 0.01$), the signal output $VM(0,4) = 1E-5$ which equals F/k (the amplitude of the driving force is one here) as it should. Also, the noise output $ONOISE(M) = 5.137E-14 \text{ m}/\sqrt{\text{Hz}}$ which equals $\sqrt{4k_B TR} / k$ as it should. At the resonance, both of these values should be Q (10) times larger and they are in the SPICE simulation.

Example B-2. Simple Accelerometer. The mechanical-impedance equivalent circuit is shown in Fig. B-6

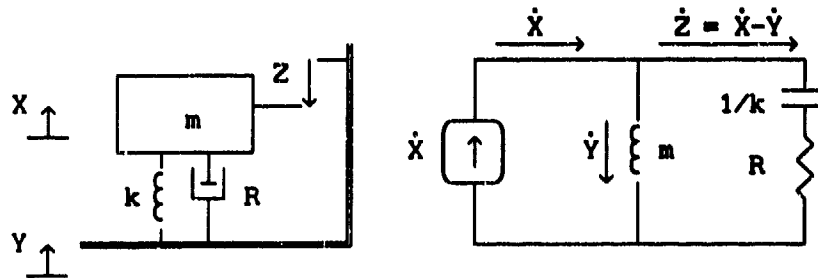


Figure B-6. Equivalent circuit for simple accelerometer.

and the electrical equivalent circuit with an input acceleration probe (LCASE) and an output displacement probe (CTEST) is shown in Fig. B-7.

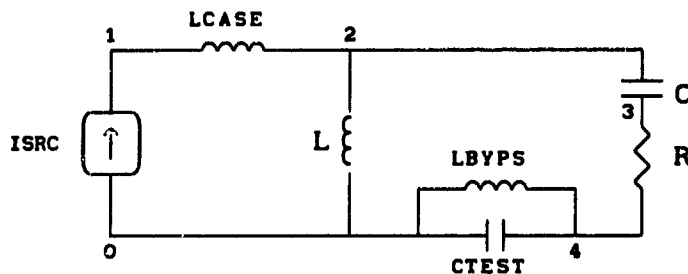


Figure B-7. SPICE equivalent circuit for accelerometer.

For normalized output as in the previous example, set CTEST = 1 and LCASE = 1. (Note: Physically, LCASE represents a small mass associated with the accelerometer case and CTEST represents a very weak spring connected between the mass pointer and the case pointer.) The other component selections are identical to those for the simple pressure sensor.

AC analysis gives the output displacement and the input acceleration. Note that, while the velocity driver is constant, the input acceleration is a function of frequency so the transfer function must be calculated by dividing the output displacement $V(0,4)$ by the input acceleration $V(2,1)$. For the pressure sensor, the input force was constant (and equal to one) so the transfer function (the sensor's

NADC-91113-50

receiving sensitivity) between input pressure and output displacement was equal to the output displacement times the transducer area. The SPICE NOISE analysis gives the thermal-noise displacement resulting from R. The following input file for SPICE performs these analyses on this circuit:

```
SIMPLE ACCELEROMETER
ISRC 0 1 AC 1 0

L      0 2 2533.03
C      2 3 1E-5
R      3 4 1591.55

LCASE 1 2 1

CTEXT 0 4 1
LBYPS 0 4 1E12

.AC DEC 10 0.01 100
.NOISE V(4,0) ISRC 20

.PRINT AC VM(1,2) VM(0,4)
.PRINT NOISE ONOISE(M)

.END
```

(The magnitude of the displacement-output to acceleration-input ratio is $VM(0,4)/VM(1,2)$.) The values for the sensor signal response and noise output from the SPICE simulation agree with the theoretical calculations.

Example B-3. Compound Accelerometer. The mechanical-impedance equivalent circuit is shown in Fig. B-8

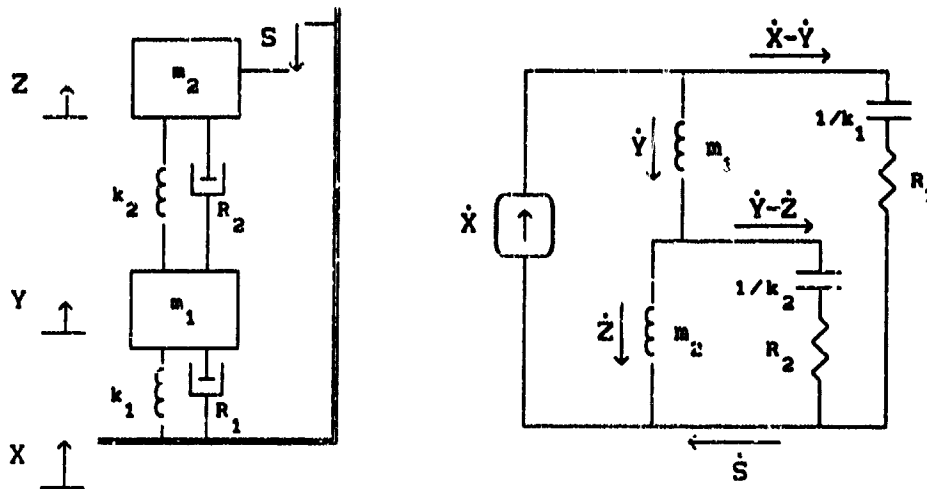


Figure B-8. Equivalent circuit for compound accelerometer.

and the electrical equivalent circuit is shown in B-9.

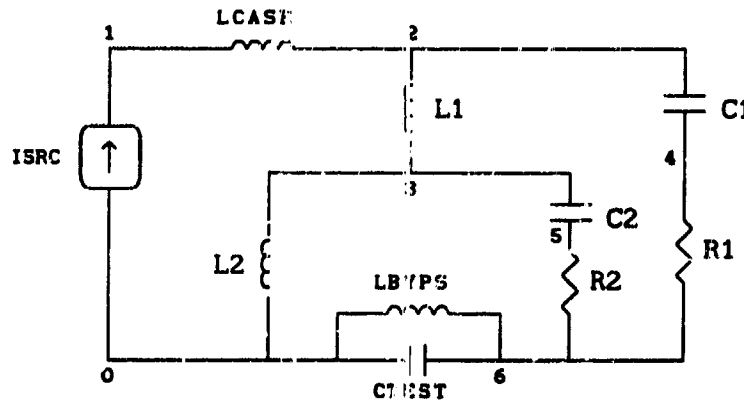


Figure B-9. SPICE equivalent circuit for compound accelerometer.

The following input file for SPICE performs the signal and noise analysis on this compound accelerometer. The values were selected so that, for the $m_1-k_1-R_1$ oscillator, the resonance frequency is one and the Q is 5; and, for the $m_2-k_2-R_2$ oscillator, the resonance frequency is two and the Q is 2.5.

NADC-91113-50

COMPOUND ACCELEROMETER
ISRC 0 1 AC 1 0

L1 2 3 2533.03
C1 2 4 1E-5
R1 4 6 3183.10

L2 3 0 1266.51
C2 3 5 1E-5
R2 5 6 3183.10

LCASE 1 2 1
CTEST 6 0 1
LBYPS 6 0 1E12

.AC DEC 10 0.01 100
.NOISE V(6,0) ISRC 20
.PRINT AC VM(1,2) VM(6,0)
.PRINT NOISE ONOISE(M)
.END

The displacement (signal) response and the noise spectral density for this compound system as calculated by the SPICE simulation are shown in Fig. B-10. Notice that the displacement response and the noise spectral density do not have the same dependence on frequency. This would introduce an error (although small in this case) in any estimate of noise power based on a measured displacement response curve.

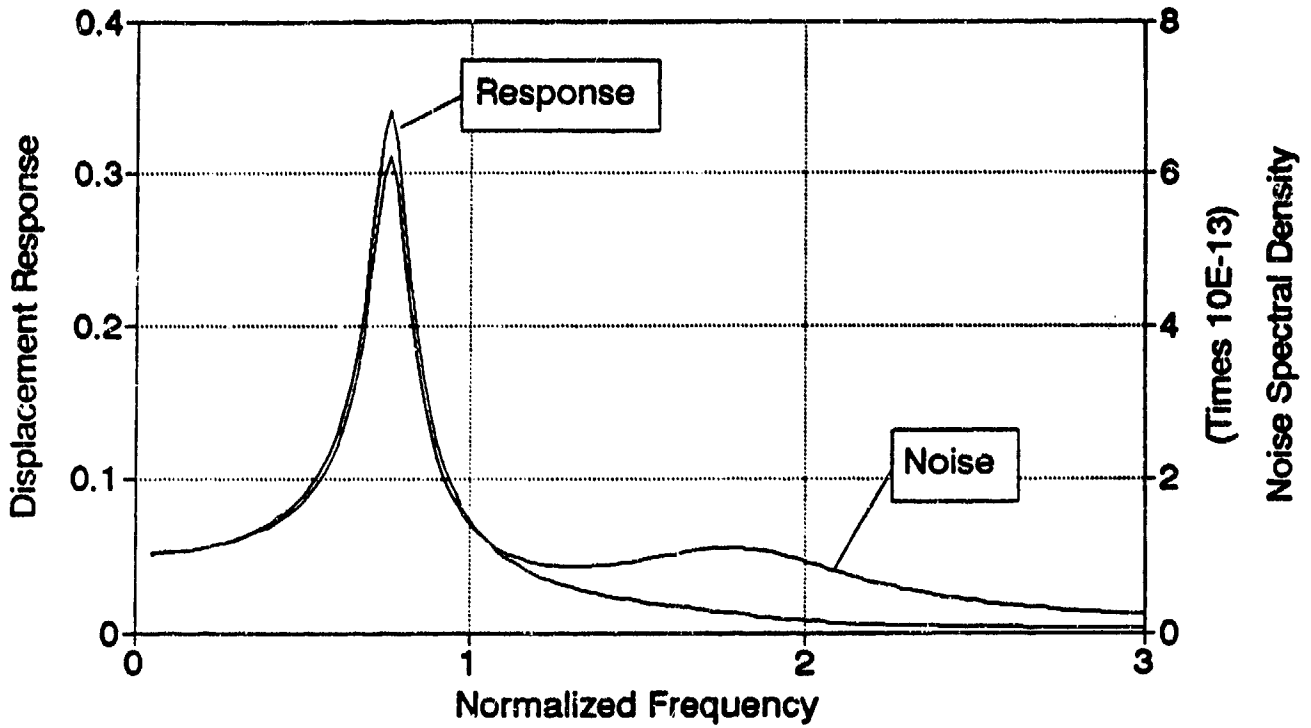


Figure B-10. Signal and noise response computed by SPICE for compound accelerometer.

Much more elaborate mechanical systems can be modeled with SPICE. With some ingenuity other forms of friction and even backlash can be described with various combinations of SPICE elements [67].

Appendix C. Noise Analysis of Op Amps and JFETs

There are several subtle problems that arise in calculating the noise of combined sensor/amplifier systems. In this Appendix, the noise characteristics of op amps and JFET preamplifiers will be considered in sufficient detail to present these problems and provide a model for analysis of similar electronic circuits.

The usual representation of noise in an amplifier or a transistor is as independent voltage and current sources. When the device is in a circuit, especially if feedback is applied, it may not be possible to maintain this independent voltage and current representation. (For example, the total noise current would contain the amplifier noise current, but the total noise voltage could also include a term resulting from the amplifier noise current flowing through a circuit resistor.) Fortunately, it is not necessary to do this. In fact, it is better to analyze the circuit with the signal source connected and calculate the total noise voltage (or the total noise current) without trying to artificially develop separate voltage and current components.

Two of the more useful techniques for performing this noise analysis are:

- (1) Compute the output voltage resulting from each noise source (amplifier current, amplifier voltage, resistor, shot) separately; divide by the circuit gain to refer the values back to the input; and, sum the squares of the individual contributions to get the total mean-square input noise voltage.
- (2) Use the signal-to-noise ratio theorem for feedback circuits [43]: The output signal-to-noise ratio is independent of the load impedance. The output SNR based on output signal and noise currents with the output shorted to ground is identical to the output SNR based on voltages with the output open-circuited. Shorting or open-circuiting the output can simplify the calculations considerably.

To illustrate these techniques, the noninverting op amp circuit will be analyzed by the first procedure and the inverting op amp will be analyzed by

the second procedure. For these analyses, the simple model for an op amp (Fig. C-1) will be used [40].

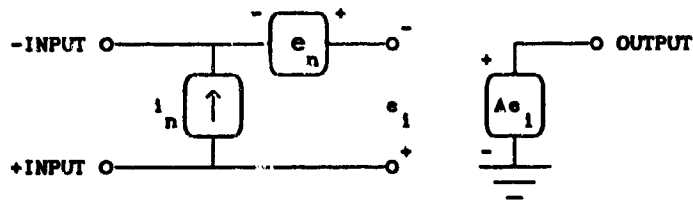


Figure C-1. Simple model for operational amplifier.

In this model, A is very large. (When the output is short-circuited to ground in the second procedure, a small series resistor representing the open-loop output impedance of the op amp will be inserted to keep the current finite.)

Noninverting Amplifier

The noninverting configuration for an operational amplifier is shown in Fig. C-2 with a source generator, e_s , and source resistance, R_s , connected.

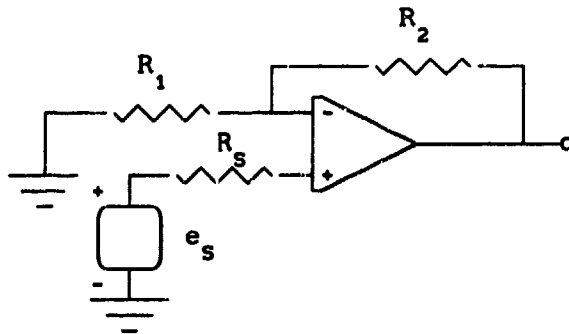


Figure C-2. Noninverting op amp circuit with source.

The noninverting configuration would normally be used with a high impedance source since the input impedance is high. The circuit model including the

resistor and amplifier noise sources is shown in Fig. C-3.

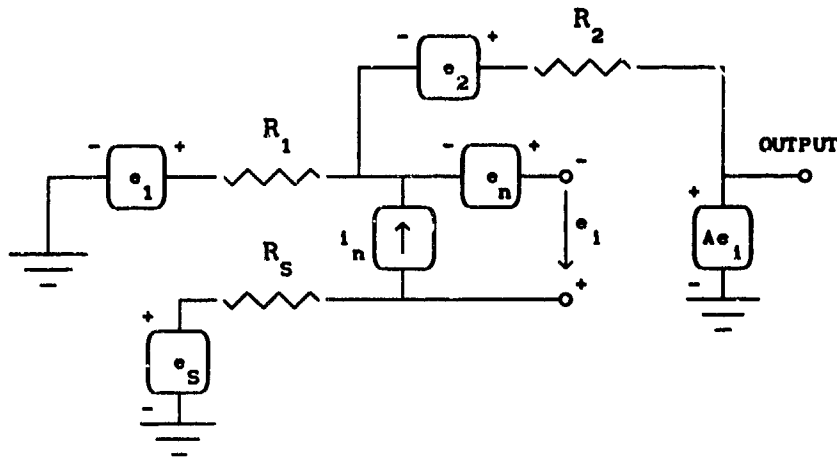


Figure C-3. Inverting op amp with source.

In this circuit, e_s can either be the noise voltage associated with R_s or the signal voltage. Since all of the noise sources (e_1 , e_2 , e_s , e_n , i_n) are assumed to be independent, consider their effects separately. Pick one source, set the others to zero (replace voltage sources by short circuits, replace current sources by open circuits), and calculate e_o (the output voltage) for each. Once this has been done for all of the noise sources, add the squares of the individual output voltages to get the total mean-square noise voltage. Calculate e_o for the signal source, square it, and divide by the total mean-square noise voltage to get the output signal-to-noise ratio. This is also the equivalent input signal-to-noise ratio for the equivalent ideal amplifier. If the equivalent input mean-square noise voltage is required, divide the total mean-square noise voltage by the circuit voltage gain squared.

For example, select e_s to analyze and set all the other sources to zero. The resulting circuit is given in Fig. C-4.

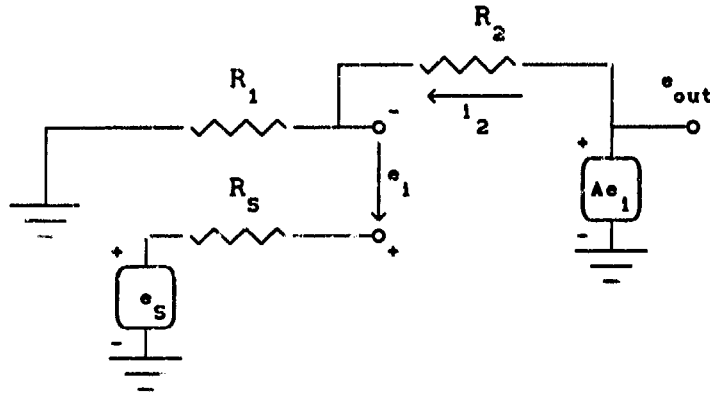


Figure C-4. Circuit of Fig. C-3 with only source generator active.

Two of the voltage loop equations are

$$i_2 R_1 + e_1 - e_s = 0 \quad (C-1)$$

and
$$e_s - e_1 + i_2 R_2 - Ae_1 = 0 \quad (C-2)$$

Eliminate i_2 , let A become very large, and solve for Ae_1 (which equals e_{out}):

$$e_{out} = Ae_1 = e_s R_2 / R_p \quad (C-3)$$

where R_p is the parallel combination of R_1 and R_2 , which equals $R_1 R_2 / (R_1 + R_2)$.

Since the source e_s can represent either the signal voltage source or the noise source of the source resistance, there are two results from this calculation. One is the signal voltage gain of the amplifier:

$$G = e_{out} / e_s = R_2 / R_p \quad (C-4)$$

The other is the mean-square noise voltage from the source resistance, which, at the output is

$$e_{out-S}^2 = 4k_B T R_s (R_2 / R_p)^2 \quad (C-5)$$

and referred back to the input is

$$e_{in-S}^2 = e_{out-S}^2 / G^2 = 4k_B T R_S \quad (C-6)$$

The other noise-voltage sources are treated similarly.

To analyze the amplifier noise current, set all other sources to zero to obtain the circuit in Fig. C-5.

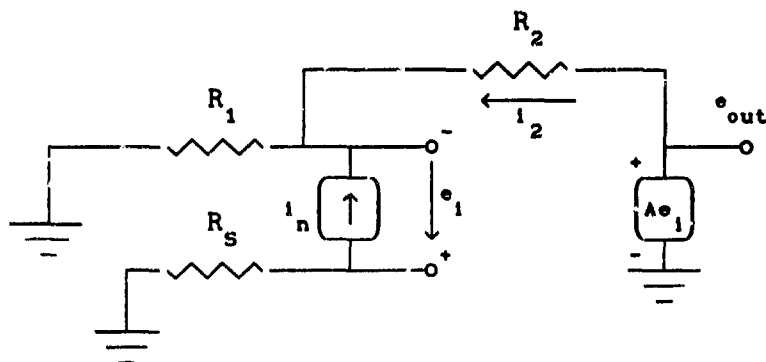


Figure C-5. Circuit of Fig. C-3 with only amplifier current noise.

Two of the loop equations are:

$$(i_n + i_2)R_1 + e_1 + i_n R_S = 0 \quad (C-7)$$

and
$$-i_n R_S - e_1 + i_2 R_2 - Ae_1 = 0 \quad (C-8)$$

Eliminate i_2 , let A become very large, and solve for Ae_1 :

$$e_{out} = Ae_1 = -i_n R_2 (1 + R_S/R_p) \quad (C-9)$$

so the mean-square noise voltage from the amplifier current noise is

$$e_{out-l}^2 = [i_n R_2 (1 + R_S/R_p)]^2 \quad (C-10)$$

at the output and

$$e_{in-l}^2 = i_n^2 (R_p + R_S)^2 \quad (C-11)$$

referred back to the input.

The output signal-to-noise ratio is equal to the voltage-squared signal output (Eq. C-3 squared) divided by the sum of the voltage-squared noise outputs (two of which are given by Eqs. C-5 and C-10). For all of the noise sources, the output signal-to-noise ratio for this circuit is then

$$\text{SNR}_{\text{out}} = \frac{e_s^2}{[e_n^2 + 4k_B T(R_S + R_p) + i_n^2(R_p + R_S)^2]} \quad (\text{C-12})$$

This is also the equivalent input signal-to-noise ratio and the denominator is the mean-square noise voltage referred to the input.

Note: In general, the source has a complex impedance, not just a resistance. The thermal noise generated directly by that impedance is only generated by the real part so, in the noise terms that are of the form $4k_B T R$, only the real part of the source impedance should be used. However, in those terms that result from currents flowing through the source impedance (resulting from, for example, e_n or i_n), the resulting voltage depends on the magnitude of the impedance and so $|Z_S|$ should be used in place of R_S .

Inverting Amplifier

The inverting configuration for an operational amplifier with a source attached is shown in Fig. C-6.

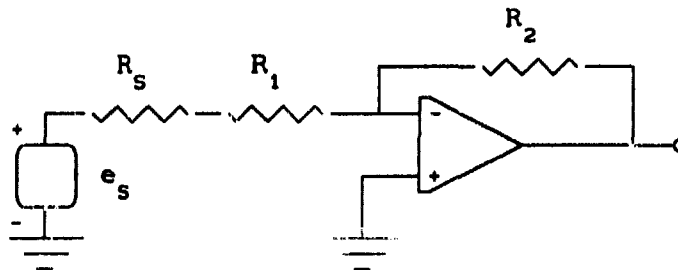


Figure C-6. Inverting configuration for op amp.

This configuration would normally be used with a low-impedance source since the input impedance is low. Figure C-7 illustrates the circuit model including the resistor and amplifier noise sources.

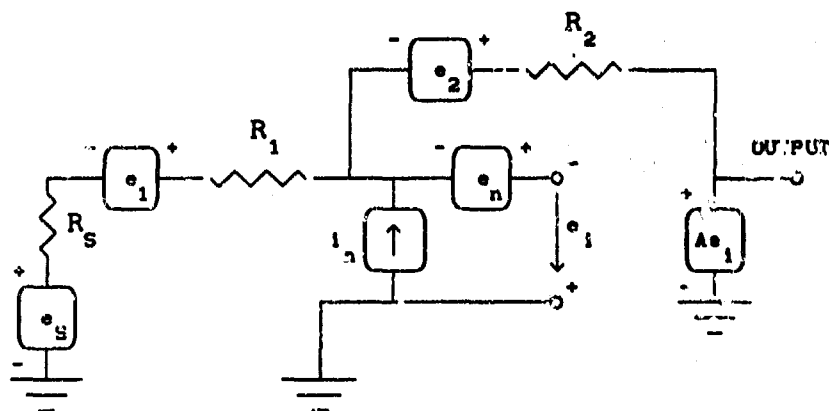


Figure C-7. Equivalent noise model for inverting op amp.

Obviously, open-circuiting the output does not simplify the circuit — it is already open circuited, so, to proceed with this technique, short the output to ground (and insert a small resistor representing the output impedance of the op). The resulting circuit is shown in Fig. C-8.

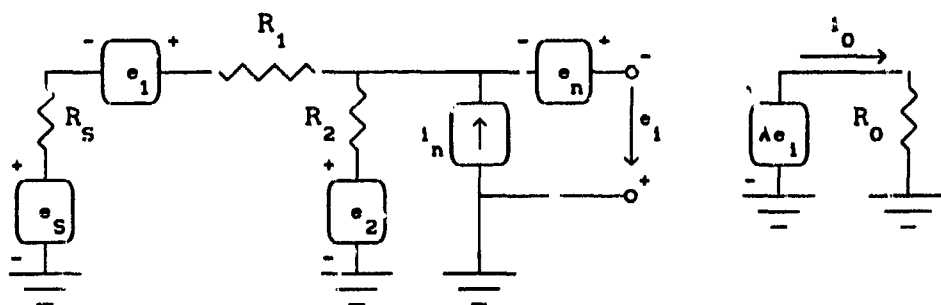


Figure C-8. Shorted-output model for inverting amplifier.

(Notice that the output current really also includes the current that flows through R_2 , but, if A is large, this contribution is negligible.)

From this point on, the solution procedure is similar to the analysis of the noninverting amplifier. First, compute the output current, i_o , for only

the signal source voltage, e_s . Squaring this gives a quantity proportional to the signal output power; this quantity will be the numerator of the signal-to-noise expression. Next, compute the individual components of noise output current by considering each noise generator separately. Finally, form the output signal-to-noise ratio by dividing the mean-square signal current by the sum of the mean-square noise components. The mean-square signal output current for this circuit is

$$i_{\text{out}}^2 = (A/R_0)^2 (e_s R_2 / R_{\text{sum}})^2 \quad (\text{C-13})$$

where $R_{\text{sum}} = R_s + R_1 + R_2$, and the output signal-to-noise ratio is

$$\text{SNR}_{\text{output}} = \frac{e_s^2}{[(R_{\text{sum}} / R_2)^2 e_n^2 + 4k_p T R_a (1 + R_a / R_2) + i_n^2 R_a^2]} \quad (\text{C-14})$$

As in the case of the noninverting amplifier, Eq. C-14 is also the input signal-to-noise ratio and the denominator is the equivalent input noise voltage. Unfortunately, the process of referring the noise to the input can cause some confusion here. The denominator of Eq. C-14 is referred to the positive terminal of the source generator, e_s . The conventional point to which the equivalent input values are referred is the node between the source resistance, R_s , and the resistor, R_1 . If it is necessary to find the equivalent voltage referred to the conventional point, the analysis should be done as for the noninverting amplifier being careful to calculate the circuit voltage gain from the proper node to the output node. However, the end result for circuit evaluations for noise is usually signal-to-noise ratio; if that is true, then it is easier to calculate the SNR directly as shown above.

(Note: The expression given in the text for the equivalent input noise voltage of the inverting amplifier is referred to the conventional node. For the noninverting amplifier, as long as the amplifier input impedance is high compared to the source impedance, this distinction is irrelevant.)

Junction Field-Effect Transistors (JFETs)

JFETs are sometimes used as the first-stage preamplifier for sensors with high source impedance. The simplified model [68] for a JFET shown in Fig. C-9 is often adequate for calculating the noise performance of a sensor/pre-amplifier combination.

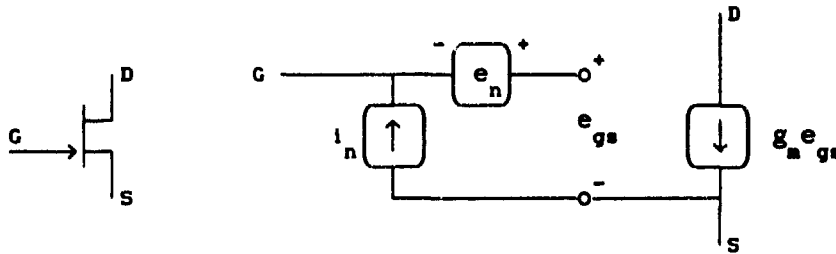


Figure C-9. Noise model for JFET.

Typical applications are as an amplifier or as a follower (Fig. C-10).

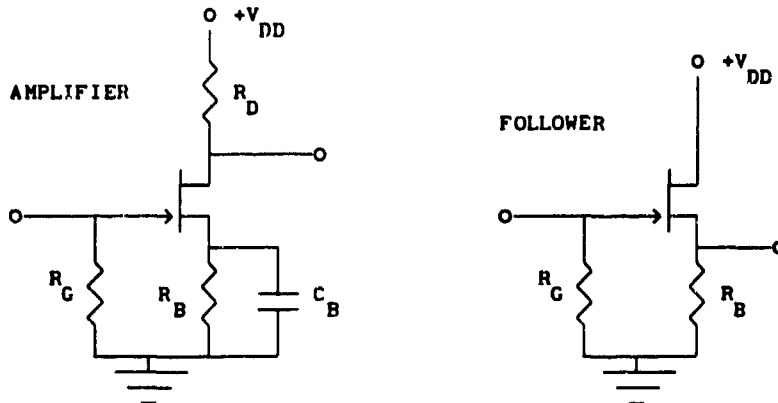


Figure C-10. Amplifier and follower applications for JFETs.

The follower is used as a high-input-impedance buffer to drive an amplifier stage, while the amplifier circuit provides some gain. In the amplifier circuit, R_B sets a DC bias point and the capacitor, C_B , effectively removes the resistor for signal frequencies.

To analyze the noise characteristics of the amplifier, connect a source generator, e_s , and its source resistance, R_s , replace the R_B - C_B combination by a short circuit, short the output to ground, and compute the signal-to-noise

ratio based on the output current. The equivalent circuit for this analysis is given in Fig. C-11.

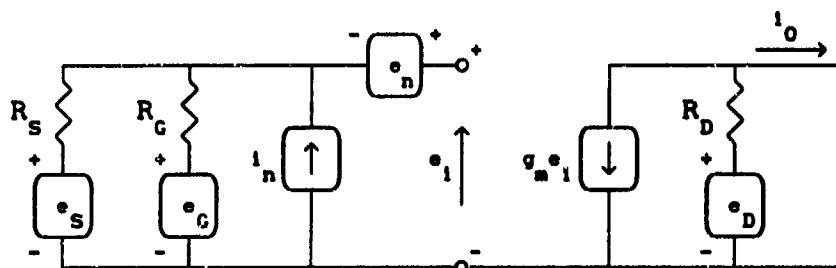


Figure C-11. Equivalent circuit for noise analysis of common-source JFET amplifier.

For signal, the output current squared is

$$i_{out}^2 = g_m^2 e_S^2 (R_p/R_S)^2 \quad (C-15)$$

where $R_p = R_S R_G / (R_S + R_G)$, while, for noise, the mean-square output current is

$$i_{out-noise}^2 = g_m^2 [e_n^2 + i_n^2 R_p^2 + 4k_B T R_p + 4k_B T R_D / (g_m R_D)^2] \quad (C-16)$$

For an amplifier, $g_m R_D > 1$, and, in the usual application, $R_D \ll R_p$, so the last term in square brackets can be neglected. The signal-to-noise ratio is Eq. C-15 divided by Eq. C-16. The equivalent mean-square noise voltage referred to the JFET gate is

$$e^2 = e_n^2 + i_n^2 R_p^2 + 4k_B T R_p \quad (C-17)$$

As discussed previously, if the source impedance is complex, then just the real part of R_p is used in the $4k_B T$ term while the magnitude of the parallel combination of the source impedance and R_G is used in the i_n^2 term.

NADC-91113-50

Microminiature sensors tend to be high-impedance devices, hence the emphasis on JFET circuits. For a low-impedance sensor, if an op amp did not provide adequate performance, a bipolar transistor input stage would be appropriate [50, 54]. The design and analysis procedures are similar although a somewhat more complicated model than was used for the JFET is usually required for the bipolar transistor.

Appendix D. Electromechanical Transducer Equivalents

A complete analysis of noise in a transducer system should consider the mechanical system coupled to the electrical system through the first stage of amplification. This Appendix reviews the equivalent circuit representation for mechanical-to-electrical transducer systems of three types: reciprocal, antireciprocal, and nonreciprocal. Once the proper equivalent circuit has been drawn, the noise analysis follows by attaching a Johnson-noise voltage generator to each resistance in the circuit.

Both the reciprocal and the antireciprocal transducers allow transduction in either direction (receiving or transmitting). While the focus here is on conversion of pressure or acceleration to voltage or current, these transducers will generate pressure or motion if a current or voltage is applied. Most conventional transducers fall into one of these categories; however, there is a very important type of transducer — the electron-tunneling sensor — in which the reverse action is governed by a different mechanism than the forward action. The reverse action is so small that the transducer can be considered to be practically unidirectional (displacement input produces current output). These nonreciprocal transducers are straightforward to model but, because a resistance corresponding to the mechanical damping does not translate over into the electrical side of the equivalent circuit, sometimes the mechanical-thermal noise is incorrectly neglected.

The reciprocal and the antireciprocal transducers can be represented by a "black-box" (Fig. D-1) in which force, F , and velocity, u , on one side are related to voltage, V , and current, I , on the other side [11]:

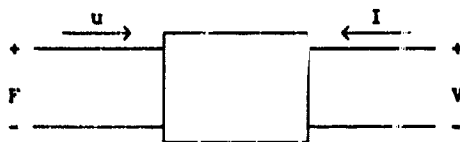


Figure D-1. Two-port representation for electromechanical transducers.

If the system is linear, the simplest general relations between the quantities are

$$\begin{aligned} V &= Z_{EB} I + T_{em} u \\ F &= T_{me} I + Z_{mo} u \end{aligned} \tag{D-1}$$

where Z_{EB} is the electrical impedance with the mechanical motion blocked ($u = 0$), Z_{mo} is the mechanical impedance with the electrical terminals open ($I = 0$), T_{em} is the transduction factor from velocity to open-circuit voltage, and T_{me} is the transduction factor from current to force when motion of the device is blocked.

If $T_{em} = T_{me}$, then the device is reciprocal. A transformation coefficient, ϕ , can be defined

$$\phi = T / Z_{EB} \tag{D-2}$$

and one way of drawing the electrical equivalent circuit, which includes the mechanical-to-electrical conversion, is shown in Fig. D-2.

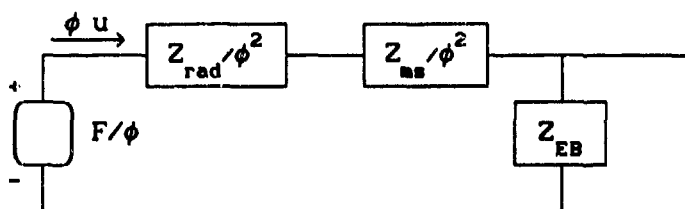


Figure D-2. Generalized equivalent circuit for reciprocal transducer.

Here, the radiation impedance, Z_{rad} , is included separately since it is often negligible. The quantity, Z_{ms} , then refers to the mechanical impedance with the electrical terminals shorted and in the absence of the radiation load.

If $T_{em} = -T_{me}$, then the transducer is antireciprocal. Another transformation coefficient, ϕ_H , can be defined:

$$\phi_H = T_{em} \tag{D-3}$$

and an equivalent circuit such as that in Fig. D-3 can be drawn.

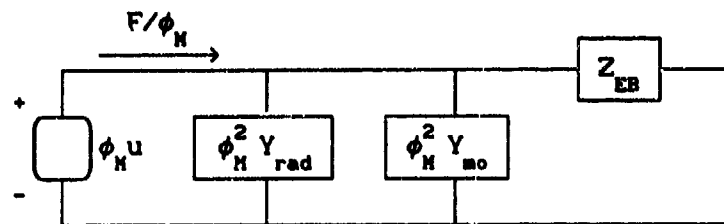


Figure D-3. Generalized equivalent circuit for anti-reciprocal transducer.

As before the radiation admittance ($Y = 1/Z$) is included separately. Notice that the mechanical voltage-like quantity is velocity and the mechanical current-like quantity is force. This switch from the normal impedance analogy was made to accommodate the antireciprocal transduction coefficients.

For reciprocal transducers, a more specific circuit (Fig. D-4) can be drawn that represents several important types [65, 69, 70]:

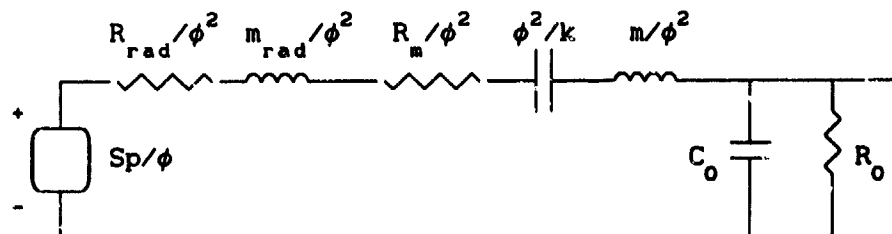


Figure D-4. Typical equivalent circuit for capacitive or piezoelectric (reciprocal) hydrophones.

This circuit can be used to analyze simple electrostatic (*i.e.*, capacitive) and piezoelectric sensors. One of the assumptions invoked to draw this circuit is that the sensor is small with respect to an acoustic wavelength so the force on the sensor face is equal to the acoustic pressure, p , times the sensor face area, S . For hydrophones operating below several tens of kilohertz, the radiation resistance is negligible; however, depending on the construction of the device, the radiation mass loading may be significant (see Appendix E). For microphones operating over high audio and ultrasonic frequencies, the radiation resistance should be included [71].

Capacitive sensors

One of the simplest reciprocal sensors is the electrostatic or capacitive sensor [11]. Two parallel plates, each of area S , are spaced a distance, x , apart and a polarizing voltage is applied. When the plate spacing changes because of an applied pressure, the charge on the plates changes, which is sensed electrically. In the following discussion, it will be assumed that the polarization circuit has no effect on the noise of the sensor. (The resistor — typically very large — in series with the polarization supply is effectively in parallel with R_0 so the electrical-thermal noise is slightly reduced.)

The capacitance, C_0 , and the transformation coefficient, ϕ , are given by

$$C_0 = \epsilon S / x_0 \quad (D-4)$$

$$\phi = C_0 V_0 / x_0 \quad (D-5)$$

where ϵ is the permittivity of the material between the plates, x_0 is the spacing between the plates with no pressure applied, and V_0 is the polarization voltage. The resistance, R_0 , can be measured or, if the loss tangent is known for the dielectric, calculated.

The mass can be calculated by adding the mass of the moveable plate (or membrane) to the radiation mass (see section on radiation impedance). Then the resonance frequency and Q can be measured with the electrical terminals shorted to get the mechanical resistance and the spring constant. If the moveable plate is a membrane and the membrane tension \mathcal{T} is known, then the stiffness, k , is $8\pi\mathcal{T}$. Alternately, if the receiving sensitivity as a function of frequency can be measured, then the mechanical parameters can be inferred from those measurements combined with an analysis of the equivalent circuit.

Piezoelectric sensors

Piezoelectric sensors are similar to capacitive sensors in that an applied strain produces a charge redistribution. There are, however, many more configurations in which piezoelectric material can be used, the choice depending on the application. Here, three common configurations will be considered: a hydrostatic-mode sensor, a cylinder, and a bender-disk. The values in the equivalent circuit will, in general, be different for each configuration but the form of the circuit will be the same or very close to that used for the capacitive sensor.

The hydrostatic-mode sensor is simply a rectangular block of piezoceramic with electrodes on one pair of opposing faces [65]. Pressure acts uniformly on all sides, the mechanical response is stiffness-dominated, and the device can tolerate very large pressure loads. Unfortunately, this configuration has rather low sensitivity.

The same equivalent circuit can be used as was used for the capacitance sensor (and the mechanical mass can be neglected). The capacitance, C_0 , and the transformation coefficient, ϕ , are given by

$$C_0 = \epsilon_{33}^S S / t \quad (D-6)$$

$$\phi = C_0 h_{33} \quad (D-7)$$

where ϵ_{33}^S is the dielectric constant for zero strain, t is the block thickness from electrode to electrode, S is the surface area of one electrode, and h_{33} is the rate of change of the electric field with applied strain for constant electric flux density. (The 33 subscript refers to the relationship between the direction of the field from electrode to electrode and the direction in which the material was polarized: For the 33-mode, these directions are the same. These parameters can be found in numerous references on piezoelectric materials, for example [65, 72].)

The mechanical stiffness, k_m , is

$$k_m = S / [t(s_{11} + 2s_{12})] \quad (D-8)$$

where the s_{12} and s_{11} are piezoceramic elastic constants. Since the transducer is very stiff, the radiation mass loading would normally be negligible; since this configuration is normally only used as a hydrophone, the radiation resistance loading can be neglected as well. Under these conditions, the open-circuit receiving sensitivity is

$$M_o = (g_{33} + 2g_{31}) t \quad (D-9)$$

where the g 's are the rates of change of electric field with respect to changes in applied stress for constant electric flux density. (Usually, g_{31} is about half of g_{33} and of the opposite sign so the "hydrostatic" sensitivity is low.) If the loss tangent of the piezoceramic material is known, then R_o can be calculated.

Higher sensitivities can be obtained by isolating one or more faces of the material from the acoustic pressure. This is often accomplished by using an air cavity. One such configuration is a cylinder of piezoceramic material with end caps and air inside. For a cylinder of length, h , radius, a , and thickness, t , the mechanical mass, m , is $\rho 2\pi a h t$ where ρ is the density of the ceramic. The applied force, F , is equal to the acoustic pressure times the surface area, $2\pi a h$.

If the cylinder is polarized parallel to the cylinder axis and the electrodes are on the inner and outer surfaces of the cylinder, then the device is being operated in the 3-1 mode [65, 73]. The capacitance, C_o , in this case is

$$C_o = \epsilon_{31}^S 2 \pi a h / t \quad (D-10)$$

and the mechanical stiffness is

$$k_m = 2 \pi h t / a s_{11}^E \quad (D-11)$$

The transformation coefficient is

$$\phi = d_{31} 2 \pi h / s_{11}^E \quad (D-12)$$

and the mechanical resistance is best determined by measuring the Q with the electrical terminals shorted.

An even simpler configuration that is air-backed is the bender disk. A thin piezoceramic disk is cemented to a brass disk that is, in turn, edge mounted over an air-filled cavity [73]. Most often, two such disks are mounted back-to-back with an edge ring to separate them and to form the cavity. If the brass disk (radius, a, and thickness, t) dominates the mass and stiffness, then the mechanical stiffness is

$$k_m = 3 \pi Y t^3 / 2 a^2 \quad (D-13)$$

where Y is the Young's modulus of the brass disk, and the mechanical mass is

$$m = 2 \pi a^2 t \rho / 3 \quad (D-14)$$

where ρ is the density of the disk. The effective water mass should be added to get the total mass. This additional mass is

$$m_w = 0.4 \pi a^3 \rho_{\text{water}} \quad (D-15)$$

The capacitance, C_0 , is

$$C_0 = \epsilon_{33}^S S / t \quad (D-16)$$

Since the disk does not move as a rigid piston, Eq. D-14 is less than the total mass of the disk. This also complicates the calculation of ϕ so that quantity should be obtained from the measured pressure response of the device. The losses can be determined from the measured Q.

Moving-coil sensors

The moving-coil sensor is the archetypical antireciprocal transducer. Because the output is proportional to the velocity of the proof mass rather

than its displacement, it is more convenient to use the mobility analog (velocity \longleftrightarrow voltage; force \longleftrightarrow current) for the mechanical parts of the circuit. A generic equivalent circuit for those moving-coil devices (for example, [22]) is shown in Fig. D-5.

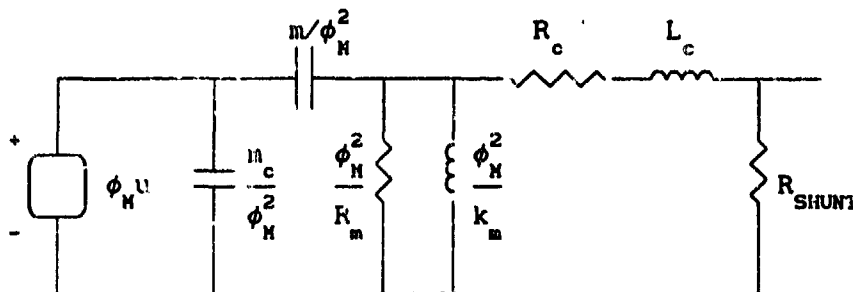


Figure D-5. Equivalent circuit for a moving-coil sensor.

The mass-spring oscillator is represented by m , R_m , and k_m ; the electrical properties of the coil by R_c and L_c ; and the mass of the sensor case by m_c . The shunt resistor is used to adjust the damping of the sensor and is usually connected externally. If the radiation load is not negligible, it can be added in parallel with the velocity generator as in Fig. D-6.

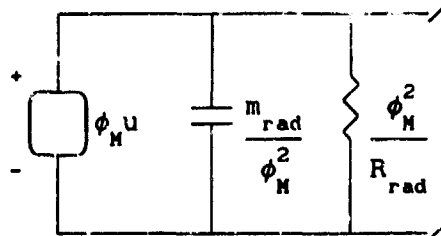


Figure D-6. Addition of radiation load for anti-reciprocal sensor.

If the sensor case moves at the same speed as the medium in which it is placed, then the velocity source is appropriate. This would be true for a small sensor attached to a massive object (a geophone in the ground or an accelerometer on a piece of machinery) or for a sensor that is neutrally buoyant and not near resonance (an accelerometer being used as a hydrophone). The more general case of an immersed sensor is better treated by using a force generator proportional to the net force resulting from the pressure integrated over the sensor case (see Appendix E).

The transformation coefficient is

$$\phi_M = B l \quad (D-17)$$

where B is the magnetic flux density (webers/m²) and l is the length of wire in the coil. Normally, B is rather hard to determine; fortunately, ϕ_M can be measured [22]:

- (1) Fix the case to a nonmoving surface ($u = 0$).
- (2) Remove the shunt resistor, R_{SHUNT} .
- (3) Measure the open-circuit damping, b_o . The mechanical resistance, R_m , can be determined from b_o .
- (4) Reconnect the shunt resistor.
- (5) Measure the damping, b_t .
- (6) If the coil inductance, L_o , can be neglected, then the transformation coefficient is

$$\phi_M^2 = 2 \omega_o m (R_c + R_{SHUNT}) (b_t - b_o) \quad (D-18)$$

Electron-tunneling sensors

For most transducers, the magnitude of the output voltage (or current) is proportional to the amount of sensing material. The capacitive sensor's output is proportional to the size of the plates, the output of a piezoceramic sensor is proportional to the amount of ceramic, and the output of a moving-coil sensor is proportional to the amount of wire and the magnetic flux density. Miniaturization necessarily reduces the sensitivity of these transducers.

An alternate means of sensing displacement is by measuring the electron tunneling current that flows between two conductors. If two conductors are very close together (on the order of a nanometer), then there is a wave-mechanical transfer of electrons from one to the other [58]. This transfer is

exponentially sensitive to the separation and so provides the basis for an extremely sensitive displacement measurement. The surface area through which the tunneling takes place need only be a few atoms in size; a larger area does not increase the sensitivity to displacement. In this sense, the electron-tunneling sensor is an ideal candidate for microminiaturization [9]. The mechanical parts of the accelerometer or pressure configuration are still subject to thermal-fluctuation motion though.

One interesting aspect of the electron-tunneling sensor is that it is effectively unidirectional. A displacement change produces a change in the tunneling current but an externally forced change in the current produces very little sensor motion. The motion produced results from electrostatic forces on the equivalent capacitance of the tunneling gap (and this capacitance is quite small) and from momentum transfer from the tunneling electrons [74]. Since these mechanisms are not the same as the mechanism for the displacement-to-voltage transduction, this device is nonreciprocal. A convenient equivalent circuit for this device is shown in Fig. D-7.

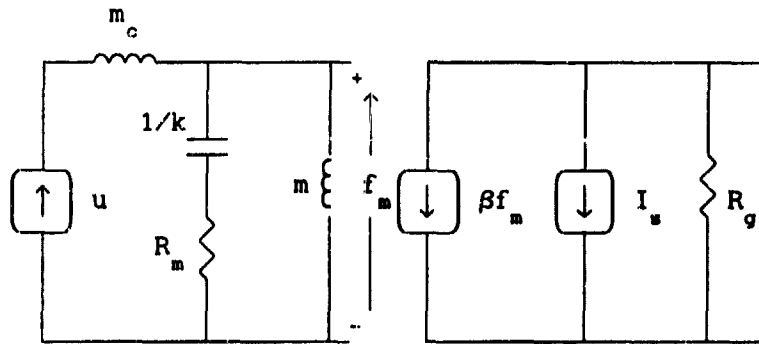


Figure D-7. Equivalent circuit for electron-tunneling sensor.

Notice that the mechanical resistance does not appear in the output branches: The thermal noise from this resistance does enter the output circuit through f_m . This would present a serious problem if the classical definition of noise figure were forced on this device since only R_g would be considered (and R_g is noiseless!). An advantage of the nonreciprocal nature is that the amplifier current noise does not feed back into the mechanical circuit so the amplifier-induced noise is not as large as it could be for a reciprocal

transducer. This advantage is inconsequential though, if the device is dominated by thermal noise in the mechanical circuit.

In the equivalent circuit given above,

$$\beta = I_0 / \omega_0^2 m x_0 \quad (D-19)$$

where I_0 is the static tunneling current (a function of the bias voltage, V_b , across the gap) and x_0 is a characteristic displacement associated with the tunneling [58]:

$$x_0 = 1 / \alpha \sqrt{\Phi} \quad (D-20)$$

where $\alpha = 1.025 \times 10^{10} \text{ m}^{-1} \text{ eV}^{-1/2}$ and Φ is the work function of the surfaces between which the tunneling is taking place (about half an electron volt for gold-to-gold tunneling). The distance, x_0 , is usually close to an angstrom. Because tunneling involves random emission of electrons across the gap, a shot noise component, $I_s = \sqrt{2qI_0}$, must also be included in the analysis along with the equivalent gap resistance, $R_g = V_b / I_0$. (Be aware that tunneling is not an equilibrium process: there is no mechanism to force the tunneling waves into equilibrium as they cross the gap so there is no thermal noise associated with R_g .) Since this device is a current generator, the first stage of preamplification is usually a high-gain current-to-voltage convertor (an inverting op amp with $R_1 = 0$).

Appendix E. Radiation Loading of Transducers

The two basic types of acoustic sensors — pressure sensors and accelerometers — differ significantly in their interaction with the medium. Most practical receiving transducers are small with respect to a wavelength in the medium over most of their operating range. If this is true, then the presence of the transducer has little effect on the acoustic waves that pass by. For a pressure sensor, this means that the relevant pressure is equal to the undisturbed acoustic pressure in the surrounding medium.

An accelerometer responds to case motion rather than pressure on the case so the appropriate quantity is the force exerted on the case by the acoustic wave. This force is equal to the integral of the pressure times the vector element of surface on the transducer case over the entire case. For a case of volume, V , with dimensions much smaller than a wavelength, the root-mean-square value of the force resulting from a traveling plane wave is

$$F = V \omega p / c \quad (\text{E-1})$$

where p is the root-mean-square acoustic pressure and c is the sound speed in the medium.

If the transducer is well represented by a rigid body with the same density as the fluid in which it is immersed (that is, if the transducer is neutrally buoyant as is common for underwater sensors), then it will move as if it were a part of the fluid. By using the above expression for force with the proper mechanical equivalent circuit, the proper case motion can be computed even if the density of the transducer is not equal to that of the surrounding fluid or if the transducer does not act like a rigid body. (At resonance, if the proof mass is of the same order as the case mass, the motion can be quite different even if the device is neutrally buoyant.)

Another difference between the pressure sensor and the accelerometer is in the radiation impedance. The pressure sensor acts as a monopole source as far as reradiation is concerned, while the accelerometer acts as a dipole

source for reradiation. A reasonable model of a small pressure transducer (for the purposes of radiation impedance calculation) is as an un baffled piston. In this case, the (mechanical) radiation impedance is [11]

$$Z_{\text{MECH}} = \rho c \pi a^2 \left[(ka)^2 / 4 + i 0.6 ka \right] \quad (\text{E-2})$$

where, here, k is the acoustic wave number (ω/c) and a is the radius of the piston. (As in the body of this paper, the convention $e^{+i\omega t}$ is used for convenience in drawing electrical equivalent circuits.)

A simple model for the reradiation of an accelerometer is that of a sphere oscillating along some axis. The radiation impedance corresponding to this motion is [30]

$$Z_{\text{MECH}} = \rho c \pi a^2 \left[(ka)^4 / 3 + i 2 ka / 3 \right] \quad (\text{E-3})$$

In comparing Eqs. E-2 and E-3, notice that the imaginary parts, representing the mass loading, are roughly equal; however, the real parts, representing the real radiation and contributing to the thermal noise, are significantly different. The dipole radiation is proportional to $(ka)^4$ which, for small ka , is much smaller than the monopole dependence of $(ka)^2$.

If the accelerometer is neutrally buoyant, the noise associated with reradiation resistance can be calculated as an equivalent pressure as is done in the text. This noise component can then be treated as an addition to the ambient noise. If the accelerometer is not neutrally buoyant (an accelerometer in air would probably not be), then Eq. E-3 should be used.

References

- [1] 1991 International Conference on Solid-State Sensors and Actuators, Digest of Technical Papers, IEEE, NY (1991)
- [2] 1990 Solid-State Sensor and Actuator Workshop Proceedings IEEE, NY (1990)
- [3] Petersen, Kurt E., "Silicon as a mechanical material," Proc. IEEE 70, 420-457 (1982)
- [4] IEEE Trans. Electron Devices ED-26(12), Special Issue on Solid-State Sensors, Actuators, and Interface Electronics (1979)
- [5] IEEE Trans. Electron Devices ED-25(10), Special Issue on Three-Dimensional Semiconductor Device Structures (1978)
- [6] Studt, Tim, "Micromachines: miniature devices come of age," Research and Development, 36-40 (Dec. 1990)
- [7] Allan, Roger, "Sensors in silicon," High Technology (Sept. 1984)
- [8] Hohm, Dietmar and Gisela Hess, "A subminiature condenser microphone with silicon nitride membrane and silicon backplate," J. Acoust. Soc. Am. 85, 476-480 (1989)
- [9] Kenny, T.W., S.B. Waltman, J.K. Reynolds, W.J. Kaiser, "Micromachined silicon tunnel sensor for motion detection," Appl. Phys. Lett. 58, 100-102 (1991)
- [10] Urick, Robert J., *Principles of Underwater Sound*, McGraw-Hill, NY (1967)
- [11] Kinsler, Lawrence E., Austin R. Frey, Alan B. Coppens, and James V. Sanders, *Fundamentals of Acoustics*, 3rd ed., Wiley, NY (1982)

NADC-91113-50

- [12] Anderson, Herbert L. (ed.), *A Physicist's Desk Reference*, AIP, NY (1989)
- [13] Sears, Francis W. and Gerhard L. Salinger, *Thermodynamics, Kinetic Theory, and Statistical Thermodynamics*, Addison-Wesley, Reading, MA (1975)
- [14] Crawford, Frank S., "Elementary derivation of the law of equipartition of energy," *Am. J. Phys.* 55, 180-182 (1987)
- [15] Einstein, A., *Investigations on the Theory of Brownian Movement*, Dover, NY (1956)
- [16] Callen, Herbert B. and Theodore A. Welton, "Irreversibility and generalized noise," *Phys. Rev.* 83(1), 34-40 (1951)
- [17] Kittel, Charles, *Elementary Statistical Physics*, Wiley, NY (1958)
- [18] Robinson, F. N. H., *Noise and Fluctuations in Electronic Devices and Circuits*, Clarendon Press, Oxford (1974)
- [19] Pippard, A. B., *The Physics of Vibration*, Cambridge University Press, NY (1989)
- [20] Johnson, J. B., "Thermal agitation of electricity in conductors," *Phys. Rev.* 32, 97- (1928)
- [21] Nyquist, H., "Thermal agitation of electric charge in conductors," *Phys. Rev.* 32, 110-113 (1928)
- [22] Mark Products, U. S. Inc., Geophone general information brochure, Houston, TX
- [23] Geospace Corp., Geospace geophones brochure, Houston, TX

- [24] Griffin, W. S., H. H. Richardson, and S. Yamanami, "A study of fluid squeeze-film damping," *Trans. ASME 88D, J. of Basic Eng.*, 451-456 (1966)
- [25] Sadd, Martin H. and A. Kent Stiffler, "Squeeze-film dampers: amplitude effects at low squeeze numbers," *Trans. ASME 97B, J. of Eng. for Industry*, 1366-1370 (1975)
- [26] Starr, James B., "Squeeze-film damping in solid-state accelerometers," *Solid-State Sensor and Actuator Workshop, Technical Digest, IEEE, NY* (1990)
- [27] Bergqvist, J., F. Rudolf, J. Maisano, F. Parodi, and M. Rossi, "A silicon condensor microphone with a highly perforated backplate," 1991 *International Conference on Solid-State Sensors and Actuators, Digest of Technical Papers, IEEE, NY* (1991)
- [28] Landau, L. D. and E. M. Lifshitz, *Fluid Mechanics*, Pergamon, NY (1984)
- [29] Lamb, Horace, *Hydrodynamics*, Dover, NY (1945) §339
- [30] Morse, Philip M. and K. Uno Ingard, *Theoretical Acoustics*, Princeton Univ. Press, Princeton (1986)
- [31] Hunt, F.V., "Thermal noise in the acoustic medium," in *AIP Handbook* (McGraw-Hill, NY, 1963) 2nd ed., pp. 3-56 to 3-59 (§3c-11)
- [32] Mellen, Robert H., "The thermal-noise limit in the detection of underwater acoustic signals," *J. Acoust. Soc. Am.* 24(5), 478-480 (1952)
- [33] van der Ziel, A., "Flicker noise in electronic devices," *Adv. Electr. Electron Phys.* 49, 225-297 (1979)
- [34] Misner, Charles W., Kip S. Thorne, and John Archibald Wheeler, *Gravitation*, W. H. Freeman, NY (1973)

- [35] Marcuse, Dietrich, *Principles of Quantum Electronics*, Academic Press, NY (1980)
- [36] MacDonald, D. K. C., *Noise and Fluctuations: An Introduction*, John Wiley and Sons, NY (1962)
- [37] Dekker, A.J., H. Hickman, T.M. Chen, "A tutorial approach to the thermal noise in metals," *Am. J. Phys.* 59, 609-613 (1991)
- [38] Caves, Carlton M., "Quantum limits on noise in linear amplifiers," *Phys. Rev. D* 26, 1817-1839 (1982)
- [39] Giffard, R. P., "Ultimate sensitivity limit of a resonant gravitational wave antenna using a linear motion detector," *Phys. Rev. D* 14, 2478-2486 (1976)
- [40] Horowitz, Paul and Winfield Hill, *The Art of Electronics*, 2nd Edition, Cambridge University Press, NY (1989)
- [41] van der Ziel, Aldert, *Noise in Measurements*, John Wiley and Sons, NY (1976)
- [42] Braddick, H. J. J., *The Physics of Experimental Method*, Chapman and Hall, London (1966)
- [43] van der Ziel, Aldert, *Noise*, Prentice-Hall, NY (1954)
- [44] Gardner, D. L., T. Hofler, S. R. Baker, R. K. Yarber, and S. L. Garrett, "A fiber-optic interferometric seismometer," *J. Lightwave Tech.* LT-5, 953 (1987)
- [45] Garrett, Steven L., "Thermal noise in simple electrical and mechanical devices," *J. Acoust. Soc. Am.* 88(S1), S159 (1990)

- [46] Mandelbrot, Benoit B. and James R. Wallis, "Some long-run properties of geophysical records," *Water Resources Res.* 5(2), 321-340 (1969)
- [47] Voss, Richard F. and John Clarke, "'1/f noise' in music: Music from 1/f noise," *J. Acoust. Soc. Am.* 63, 258-263 (1978)
- [48] Dutta, P. and P. M. Horn, "Low-frequency fluctuations in solids: 1/f noise," *Rev. Mod. Phys.* 53, 497-516 (1981)
- [49] Weissman, M. B., "1/f noise and other slow, nonexponential kinetics in condensed matter," *Rev. Mod. Phys.* 60, 537-571, (1988)
- [50] Motchenbacher, C. D. and F. C. Fitchen, *Low-Noise Electronic Design*, Wiley, NY (1973)
- [51] Ngo, Kim Chi Thi, "Measurement of thermal noise in condensor microphones in a vacuum-isolation vessel," MSEE Thesis, Old Dominion University, VA (Nov. 1990)
- [52] Zuckerwar, Allan J. and Kim Chi T. Ngo, "Wideband measurements of thermal noise in condensor microphones," *J. Acoust. Soc. Am.* 88(S1), S161 (1990)
- [53] Ngo, Kim Chi T. and Allan J. Zuckerwar, "Vacuum isolation vessel for measurement of thermal noise in microphones," *J. Acoust. Soc. Am.* 88(S1), S161 (1990)
- [54] Netzer, Yishay, "The design of low-noise amplifiers," *Proc. IEEE* 69, 728-741 (1981)
- [55] Analog Devices, *Linear Products Databook*, Norwood, MA (1988)
- [56] National Semiconductor, *Linear Databook*, Santa Clara, CA (1980)
- [57] Linear Technology, "LT1028 Data Sheet," Milpitas, CA (1989)

- [58] Binnig, G. and H. Rohrer, "Scanning tunneling microscopy," *IBM J. Res. Develop.* 30, 355-369 (1986)
- [59] Marton, L. and W.F. Hornyak, *Methods of Experimental Physics, Vol. 8*, Academic Press, NY (1969)
- [60] Hofler, Thomas J. and Steven L. Garrett, "Thermal noise in a fiber optic sensor," *J. Acoust. Soc. Am.* 84(2), 471-475 (1988)
- [61] Mermelstein, Marc D., "Comment on "Thermal noise in a fiber optic sensor" [*J. Acoust. Soc. Am.* 84, 471-475 (1988)]" *J. Acoust. Soc. Am.* 87, 1362-1363 (1990)
- [62] Gradshteyn, I. S. and I. M. Ryzhik, *Table of Integrals, Series, and Products*, Academic Press, NY (1980)
- [63] Pauli, Wolfgang, *Pauli Lectures on Physics: Volume 4. Statistical Mechanics*, MIT Press, Cambridge, MA (1973)
- [64] Longair, M. S., *Theoretical Concepts in Physics*, Cambridge University Press, Cambridge (1984)
- [65] Wilson, O. B., *An Introduction to the Theory and Design of Sonar Transducers*, USGPO, Washington, DC (1985)
- [66] Tuinenga, P., *Spice: A Guide to Circuit Simulation and Analysis Using PSpice*, Prentice-Hall, Englewood Cliffs, NJ (1988)
- [67] Bello, Vincent G., "Electrical models of mechanical units widen simulator's scope," *EDN* 36(7), 139-144 (28 March 1991)
- [68] Angelo, E. James Jr., *Electronics: BJTs, FETs, and Microcircuits*, McGraw-Hill, NY (1969)

- [69] Woollett, Ralph S., "Procedures for comparing hydrophone noise with minimum water noise," J. Acoust. Soc. Am. 54, 1376-1379 (1973)
- [70] Young, J.W., "Optimization of acoustic receiver noise performance," J. Acoust. Soc. Am. 61, 1471-1476 (1977)
- [71] Olsen, Harry F., "Microphone thermal agitation noise," J. Acoust. Soc. Am. 51, 425-432 (1972)
- [72] Channel Industries, Catalog 761-01, Santa Barbara, CA
- [73] Butler, John L., "Underwater sound transducers," unpublished notes, Image Acoustics, N. Marshfield, MA (1982)
- [74] Bocko, Mark F., Kendall A. Stephenson, and Roger H. Koch, "Vacuum tunneling probe: a nonreciprocal, reduced-back-action transducer," Phys. Rev. Lett. 61, 726-729 (1988)

NADC-91113-50

Defense Technical Information Center
ATTN: DTIC-FDAB
Cameron Station BGS
Alexandria, VA 22304-6145

2

Naval Air Warfare Center
Aircraft Division
ATTN: Code 8131
T. Gabrielson (Code 5044)
Warminster, PA 18974

2

20

Scripps Oceanographic Institute
Marine Physical Laboratory
ATTN: W. Hodgkiss 1
San Diego, CA 92152

University of Texas at Austin
Department of Mechanical Engineering
ATTN: M. Hamilton 1
Austin, TX 78712-1063

Applied Research Laboratory
The Pennsylvania State University
ATTN: A. Stuart, W. Thompson, S. McDaniel 3
P. O. Box 30
State College, PA 16804

Massachusetts Institute of Technology
ATTN: I. Dyer, A. Baggeroer 2
Department of Ocean Engineering
Cambridge, MA 02139

New Jersey Institute of Technology
ATTN: Prof. W. Clemens 1
Department of Electrical Engineering
Newark, NJ 07102

Science Applications International Corp.
ATTN: A. Eller 1
P. O. Box 1303
McLean, VA 22102

Los Alamos National Laboratory
ATTN: G. Swift (MS 764) 1
W. Ward (MS J576) 1
P. O. Box 1663
Los Alamos, NM 87545

NASA Langley Research Center
ATTN: A. Zuckerwar (MS 238) 1
Hampton, VA 23665

NADC-91113-50

Charles Stark Draper Laboratory
ATTN: J. Bernstein (MS 37) 1
555 Technology Square
Cambridge, MA 02139

Triton Technologies Inc
ATTN: W. Henrion 1
1301 Capital of Texas Highway South
Austin, TX 78746

Sparton Electronics
ATTN: J. Chomic 1
2400 E. Ganson St.
Jackson, MI 49202

Sippican Ocean Systems, Inc.
ATTN: R. Bixby 1
7 Barnabas Road
Marion, MA 02738

Raytheon Company
Submarine Signal Division
ATTN: L. Livernois 1
1847 West Main Road
Portsmouth, RI 02871-1087

Hazeltine Corporation
ATTN: T. Bourgault 1
115 Bay State Dr.
Braintree, MA 02184

Hermes Electronics Limited
ATTN: J. Fortenberry 1
7881 Hampton Village Pass
Annandale, VA 22003

Dowty Maritime Systems, Ltd.
ATTN: D. Buckingham 1
419 Bridport Road
The Metropolitan Centre
Greenford Middlesex
UB6 8UA ENGLAND

Woods Hole Oceanographic Institution
ATTN: G. Frisk, J. Lynch 1
Woods Hole, MA 02543

NADC-91113-50

Superintendent
U. S. Naval Academy
Physics Department
ATTN: M. Korman 1
Annapolis, MD 21403

Loral
Defense Systems - Akron
ATTN: C. Lavan 1
1210 Massillon Road
Akron, OH 44315-0001

National Center for Physical Acoustics
ATTN: H. Bass 1
P. O. Box 847
University of Mississippi
Oxford, MS 38677

Sperry Marine Inc.
ATTN: D. Gerdt 1
1070 Seminole Trail
Charlottesville, VA 22906

Magnavox Electronic Systems Company
ATTN: G. Lewis 1
1313 Production Rd.
Ft. Wayne, IN 46808

Jet Propulsion Laboratory
Space Microelectronic Device Technology Section
ATTN: W. Kaiser, T. Kenny 3
4800 Oak Grove Drive
Pasadena, CA 91109-8099

AT&T Bell Laboratories
VLSI Systems
ATTN: A. Hartman, P. Evans, R. Perry 3
1 Whippany Road
Whippany, NJ 07981

Lawrence-Livermore National Laboratory
ATTN: L. Ng, P. Kuzmenko 2
P. O. Box 808, L-97
Livermore, CA 94551

NADC-91113-50

Distribution List

Chief of Naval Research Office of Naval Technology ATTN: T. Goldsberry (Code 231) 800 N. Quincy Street Arlington, VA 22217	3
Chief of Naval Research Office of Naval Research ATTN: L. Hargrove (Physics Division) 800 N. Quincy Street Arlington, VA 22217	1
Commanding Officer Naval Research Laboratory ATTN: J. Murday, R. Colton (Code 6100) 4555 Overlook Avenue Washington, D.C. 20375	2
Division Superintendent Naval Research Laboratory, USRD ATTN: J. Blue, R. Timme, R. Ting P. O. Box 568337 Orlando, FL 32856-8337	3
Superintendent Naval Postgraduate School ATTN: S. Garrett (Code PH/Gx) O. Wilson (Code PH/W1) A. Atchley (Code PH/Ay) D. Gardner (Code PH/Gd) Monterey, CA 93943	1 1 1 1
Officer in Charge, New London Laboratory Naval Underwater Systems Center ATTN: W. Roderick (Code 10) T. Straw (Code 432) F. Tito, J. Powers (Code 2131) R. Hauptman (Code 2142) G. Connolly (Code 2192) New London, CT 06320-5594	1 1 2 1 1
Commander Naval Ocean Systems Center ATTN: M. Morrison (Code 541) San Diego, CA 92152	1